Structure of Hypernuclei and Eos with Hyperon

Hiroyuki Sagawa University of Aizu/RIKEN

1. Introduction
2. Hyperon-Nucleon interaction and Hypernuclei
3. Structure study of hypernuclei
4. EoS with strange particle in RMF
5. Mass of Neutron stars and three-body forces

Major goals of hypernuclear physics

Courtesy of E. Hiyama

1) To understand baryon-baryon interactions (NN, YN,YY ---) in nuclear medium and nuclear matter

Fundamental and important for the study of nuclear physics

2) To study the structure of multi-strange systems

To understand the baryon-baryon interaction, two-body scattering experiment is most useful.

Total number of
Nucleon (N) -Nucleon (N) data: 4,000

- Total number of differential cross section

Hyperon (Y) -Nucleon (N) data: **40**

- **NO** YY scattering data

YN and YY potential models so far proposed (ex. Nijmegen, Julich, Kyoto-Niigata) have large ambiguity.

$$V_{\Lambda N} = V_0 + \boldsymbol{\sigma}_\Lambda \cdot \boldsymbol{\sigma}_N V_{\sigma\cdot\sigma} + \mathbf{L}\cdot(\mathbf{s}_\Lambda + \mathbf{s}_N) V_{\rm SLS} + \mathbf{L}\cdot(\mathbf{s}_\Lambda - \mathbf{s}_N) V_{\rm ALS} + S_{12} V_{\rm tensor} + \cdots\cdots$$

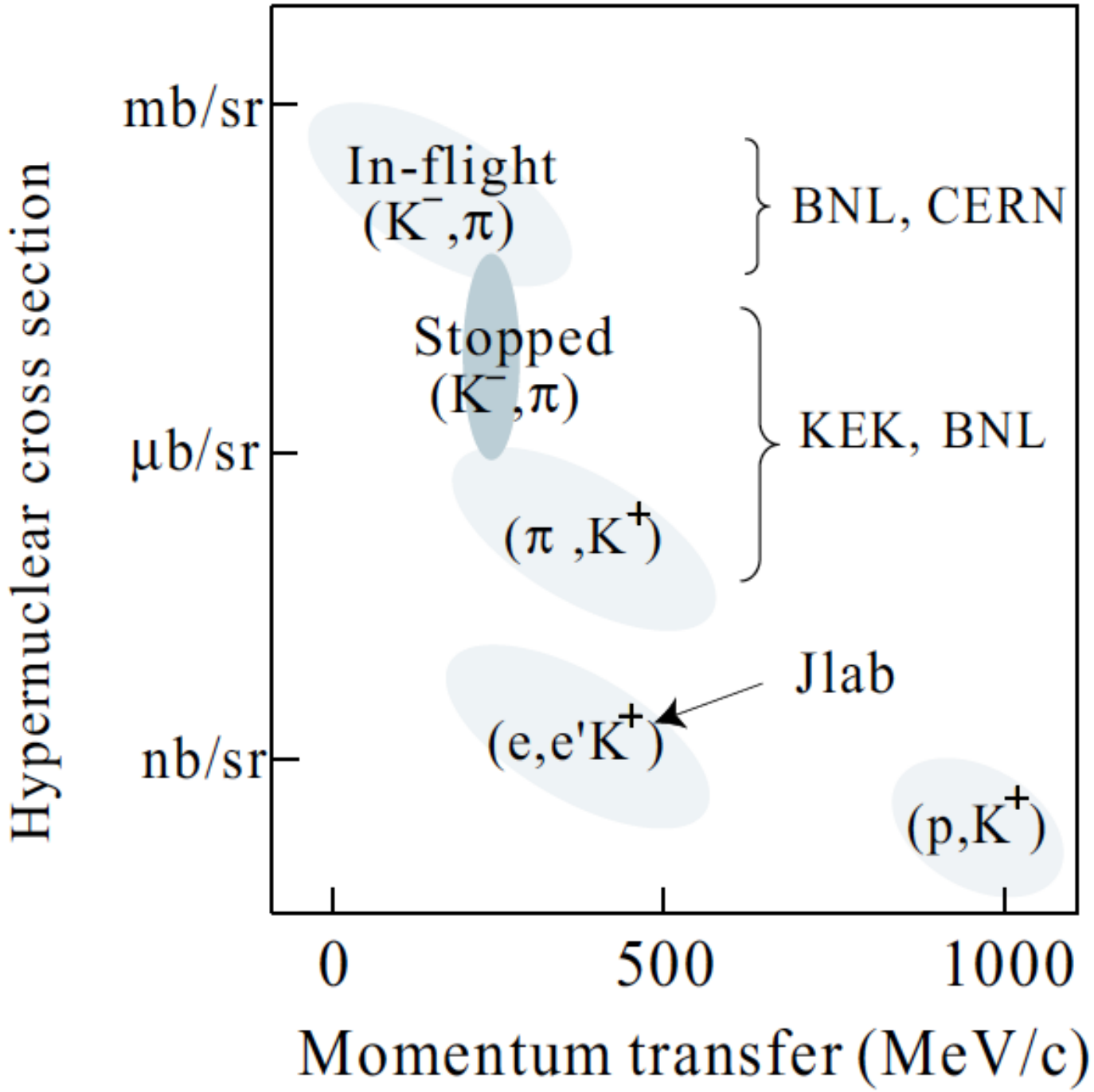
mb/sr
μb/sr
nb/sr
Hypernuclear cross section
In-flight
(K⁻,π)
BNL, CERN
Stopped
(K⁻,π)
KEK, BNL
(π ,K⁺)
Jlab
(e,e'K⁺)
(p,K⁺)
0
500
1000
Momentum transfer (MeV/c)

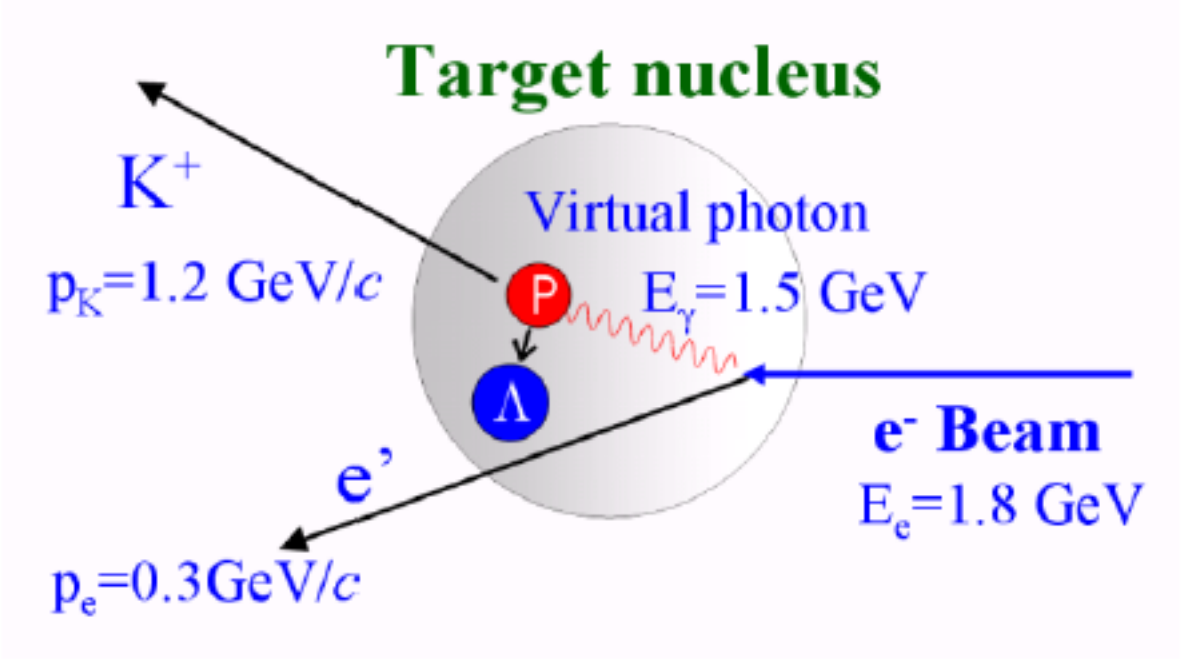

Fig. 5. Kinematical condition of the $(e, e' K^+)$ reaction for Jlab E89-009.

Jlab	Hall A and Hall C experiments energy resolution 0.5MeV high momentum transfer => good to study high spin states
Jparc	energy resolution more than 1MeV

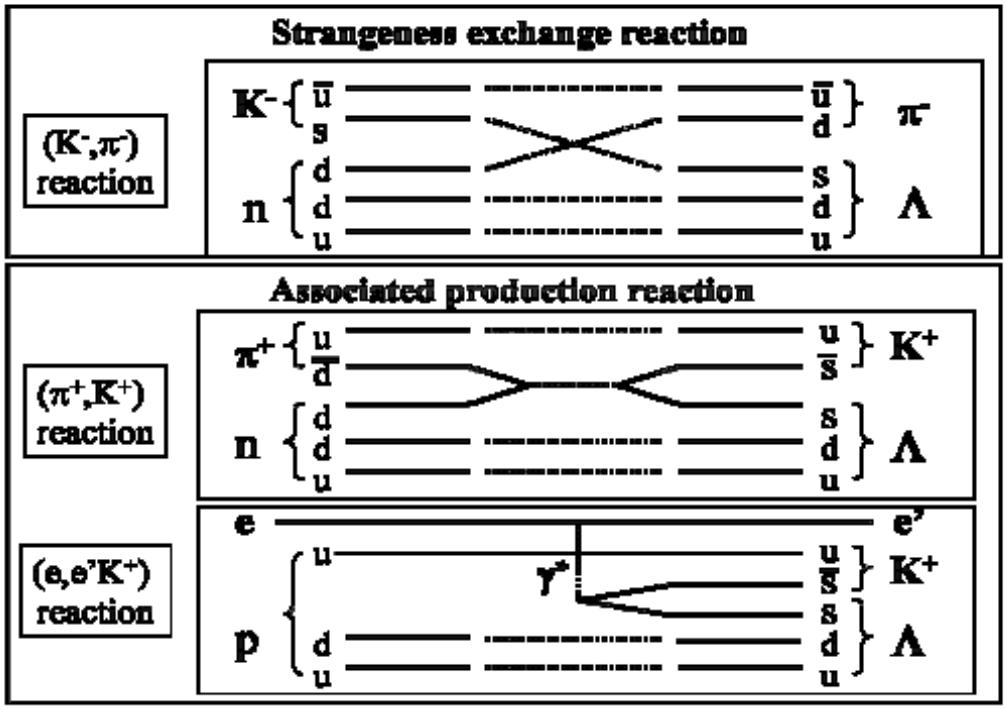

Table 1: Comparison of Λ Hypernuclear production reactions

$\Delta Z = 0$ *neutron to* Λ	$\Delta Z = -1$ *proton to* Λ	comment
(π^+, K^+)	(π^-, K^0)	stretched, high spin
in-flight (K^-, π^-) stopped (K^-, π^-)	in-flight (K^-, π^0) stopped (K^-, π^0)	substitutional
$(e, e'K^0)$ (γ, K^0)	$(e, e'K^+)$ (γ, K^+)	spin-flip, unnatural parity

Strategy to determine YN and YY interactions
from the studies of light hypernuclear structure

YN SLS+ALS potentials

Meson theory :Nijmegen
Quark model :Kyoto-Niigata

① Use

③ Suggest to improve

④ new version potential (ESC06)

Accurate calculation of energy splitting (${}^{9}_{\Lambda}$Be and ${}^{13}_{\Lambda}$C)
using the YN SLS+ALS potentials

② comparison

⑤ comparison again: good agreement

Spectroscopy experiments

High-resolution **γ**-ray spectroscopy experiment in ${}^{9}_{\Lambda}$Be and ${}^{13}_{\Lambda}$C

by Tamura and his collaborators

by Kishimoto and his collaborators

Single-particle energies of Λ

G-matrix results vs. experiments

(Y. Yamamoto et al.: Prog. Ther. Phys. S.185 (2010) 72.)

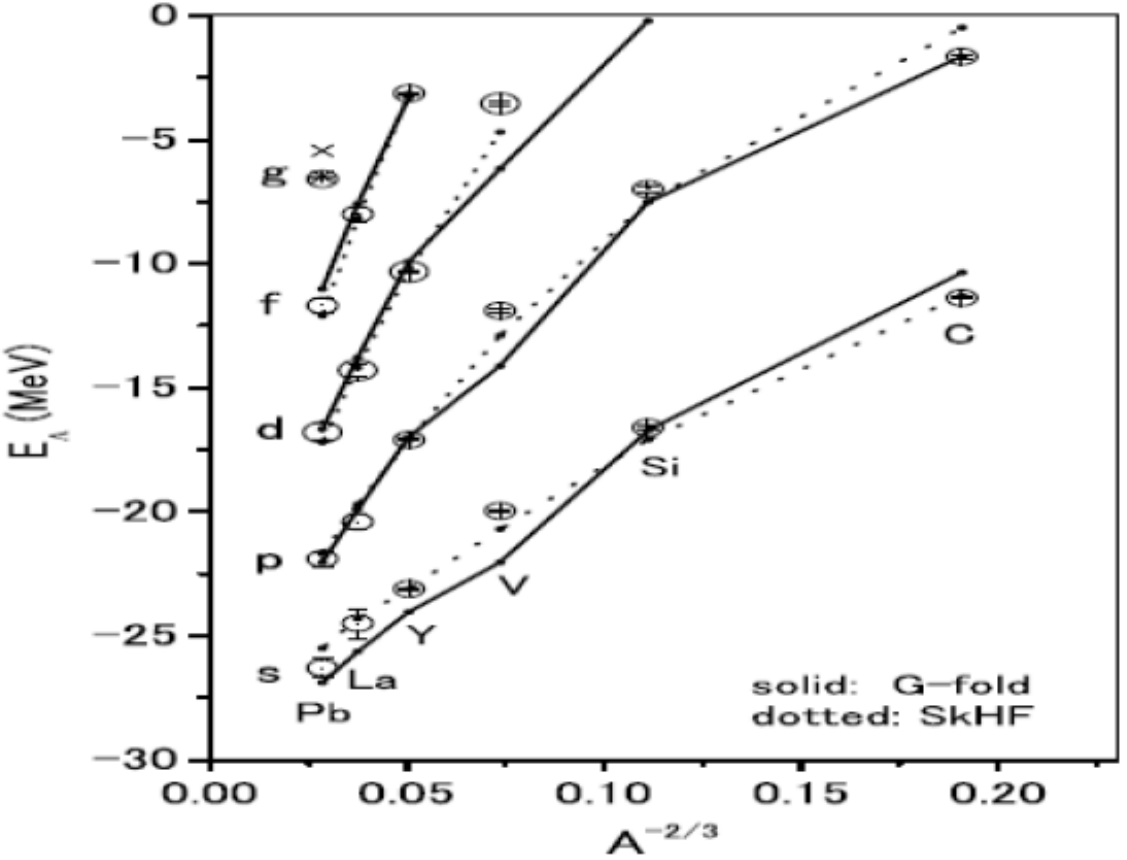

Sd- and *fp*-shell data are quite Important to extract the Λ behavior in nuclear matter.

Fig. 1. Energy spectra of ${}^{13}_{\Lambda}$C, ${}^{28}_{\Lambda}$Si, ${}^{51}_{\Lambda}$V, ${}^{89}_{\Lambda}$Y, ${}^{139}_{\Lambda}$La and ${}^{208}_{\Lambda}$Pb are given as a function of $A^{-2/3}$, A being mass numbers of core nuclei. Solid (dashed) lines show calculated values by the G-matrix folding model derived from ESC08a (the Skyrme-HF model). Open circles denote the experimental values taken from Ref. 17).

Energy levels of core nuclei and hypernuclei

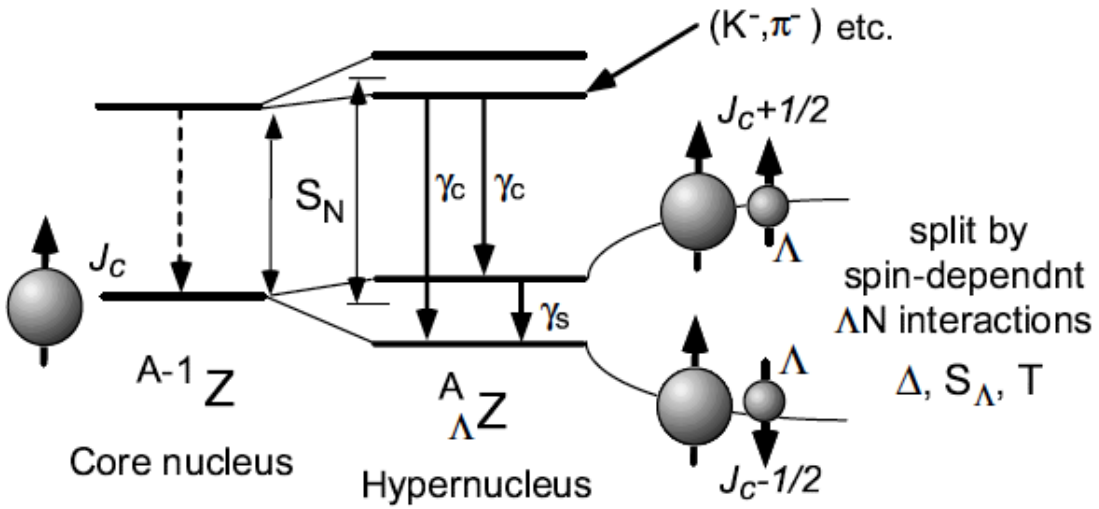

Figure 42: Schematic scheme of low-lying levels of a Λ hypernucleus and γ transitions. γ_c and γ_s are called "core transition" and "Λ-spin-flip transition", respectively. Excellent resolution of Ge detectors is essential to resolve two levels (called "hypernuclear fine structure") split by the ΛN spin-dependent interactions. See text for details.

Hypernuclear γ-ray data since 1998

Courtesy of Tamura

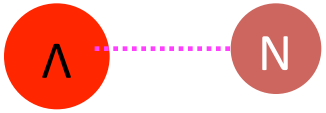

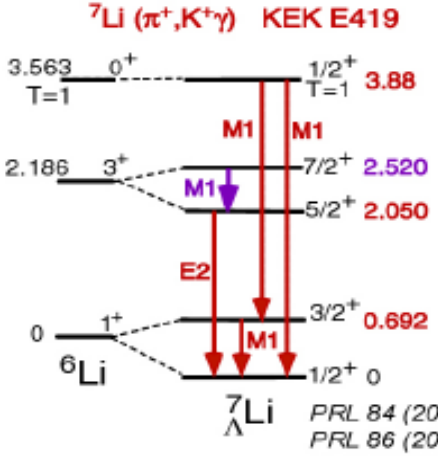

PRL 84 (2000) 5963
PRL 86 (2001) 1982
PLB 579 (2004) 258
PRC 73 (2006) 012501

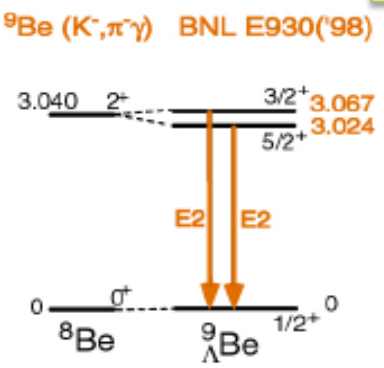

PRL 88 (2002) 082501
NPA 754 (2005) 58c

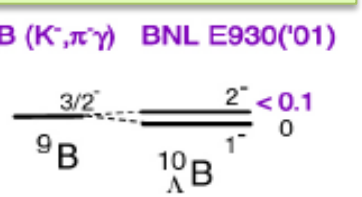

NPA 754 (2005) 58c

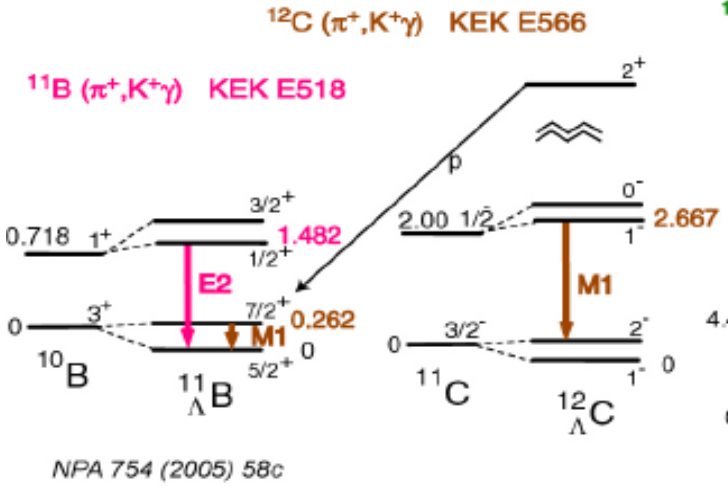

NPA 754 (2005) 58c

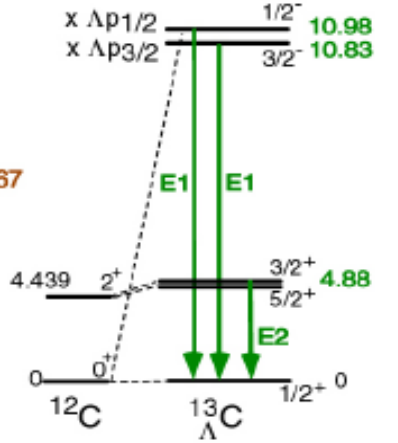

PRL 86 (2001) 4255
PRC 65 (2002) 034607

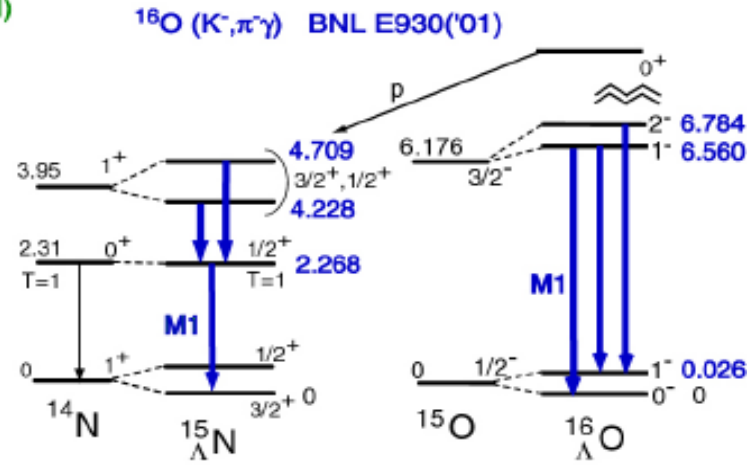

PRL 93 (2004) 232501

$$V_{\Lambda N} = V_0 + \boldsymbol{\sigma}_\Lambda \cdot \boldsymbol{\sigma}_N V_{\sigma\cdot\sigma} + \mathbf{L}\cdot(\mathbf{s}_\Lambda + \mathbf{s}_N) V_{\mathrm{SLS}} + \mathbf{L}\cdot(\mathbf{s}_\Lambda - \mathbf{s}_N) V_{\mathrm{ALS}} + S_{12} V_{\mathrm{tensor}} + \cdots\cdots$$

- Millener (p-shell model),
- Hiyama (few-body)

Hypernuclear physics

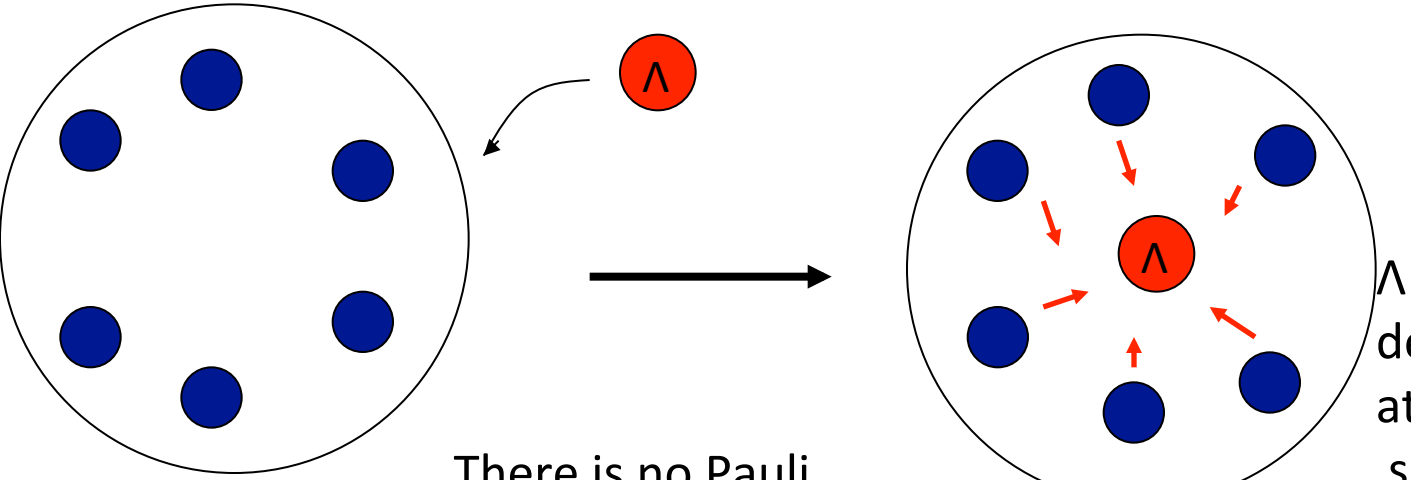

Nucleus

There is no Pauli Pricliple between N and Λ.

Hypernucleus

Λ particle can reach deep inside, and attract the surrounding nucleons towards the interior of the nucleus.

Λ particle plays a ‘glue like role’ to produce a dynamical contraction of the core nucleus.

How do we observe nuclear shrinkage effect by experiment?

Theoretical calculation by Hiyama et al.
$B(E2: 5/2^+ \rightarrow 1/2^+) = 2.85\ e^2fm^4$
$R_{\alpha\text{-}np}(^7Li)$ is reduced by 22%

KEK-E419

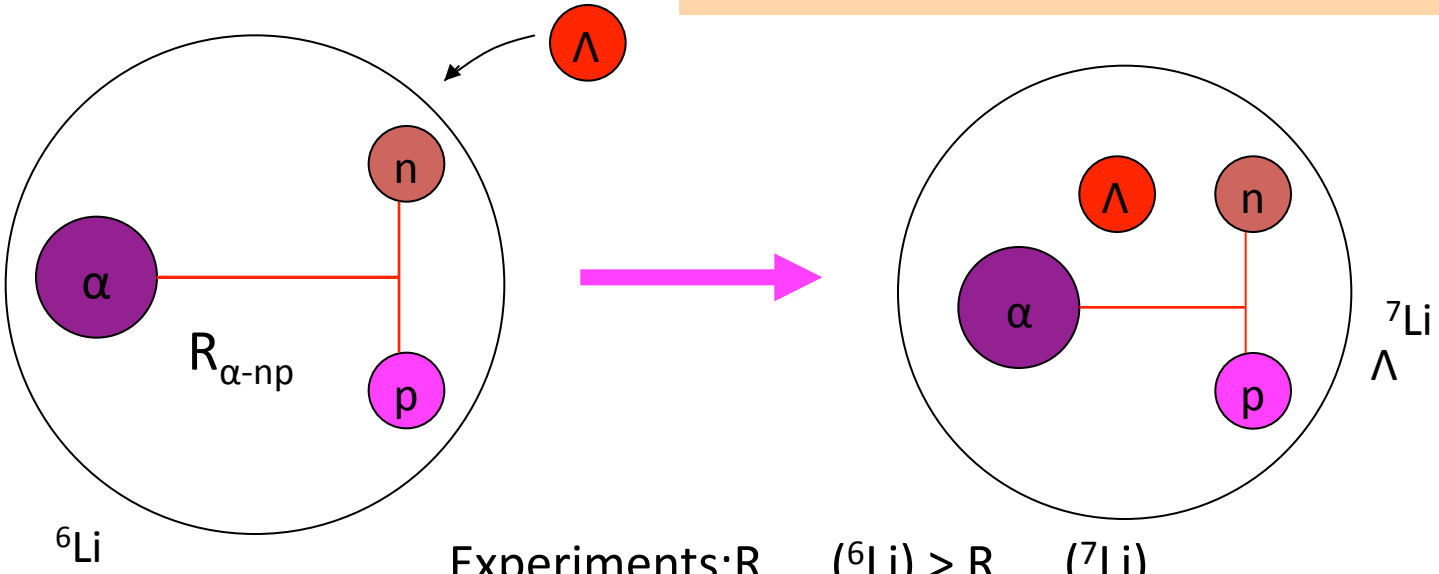

Experiments: $R_{\alpha\text{-}np}(^6Li) > R_{\alpha\text{-}np}(^7_\Lambda Li)$
reduced by about 19 %

$B(E2: 3^+ \rightarrow 1^+ : ^6Li) = 9.3 \pm 0.5\ e^2fm^4 \rightarrow B(E2: 5/2^+ \rightarrow 1/2^+ : ^7_\Lambda Li) =$ 3.6 ±2.1 e^2fm^4

$$B(E2) \propto R^4$$

The shrinkage effect on the nuclear size included by the Λ particle was confirmed for the first time.

Theoretical models for hypernuclei and EoS with hyperons

- RMF (Relativistic Hartree, Relativistic Hartree-Fock models)
- Skyrme Hartree-Fock model with hyperon
  YN interaction : SU(3) model or phenomenological
- Bruckner Hartree-Fock model with YN scattering data
- quark-coupling model
- chiral model

- Three-body interaction
  RMF: ωNY σNY
  BHF: Fujita-Miyazawa-type 3body YNN interaction
  +repulsive YNN at higher density

SHF and RMF are phenomenological models

- **Baryon one-loop approximation (Hartree approximation) makes RMF a phenomenological model.**
  → We need DATA and AB INITIO results.
  - **Saturation point (ρ_0 and $E/A(\rho_0)$) from mass formula**
  - **Nuclear binding energies**
  - **U_V and U_S from DBHF results** (RMF)
  - **$P(\rho_B)$ from heavy-ion data**

  NN part

  - **Λ separation energy from single Λ hypernuclear data**
  - **ΛΛ bond energy from double Λ hypernuclear data**
  - **Σ atomic shift**
  - **Σ and Ξ potential depth from quasi-free production data**

  YN part

- Relativistic Hartree-Fock model with pion coupling+rho tensor coupling

Vector potential in RMF

- **Vector potential from ω dominates at high density !**

$$U_v(\rho_B) = g_\omega \omega \sim \frac{g_\omega^2}{m_\omega^2}\rho_B$$

  - **Dirac-Bruckner-Hartree-Fock shows suppessed vector potential at high ρ_B.**
    R. Brockmann, R. Machleidt, PRC42('90)1965.
  - **Collective flow in heavy-ion collisions suggests pressure at high ρ_B.**
    P. Danielewicz, R. Lacey, W. G. Lynch, Science298('02)1592.
  - **Self-interaction of ω ~ $c_\omega(\omega_\mu\omega^\mu)^2$**
    → DBHF results & Heavy-ion data

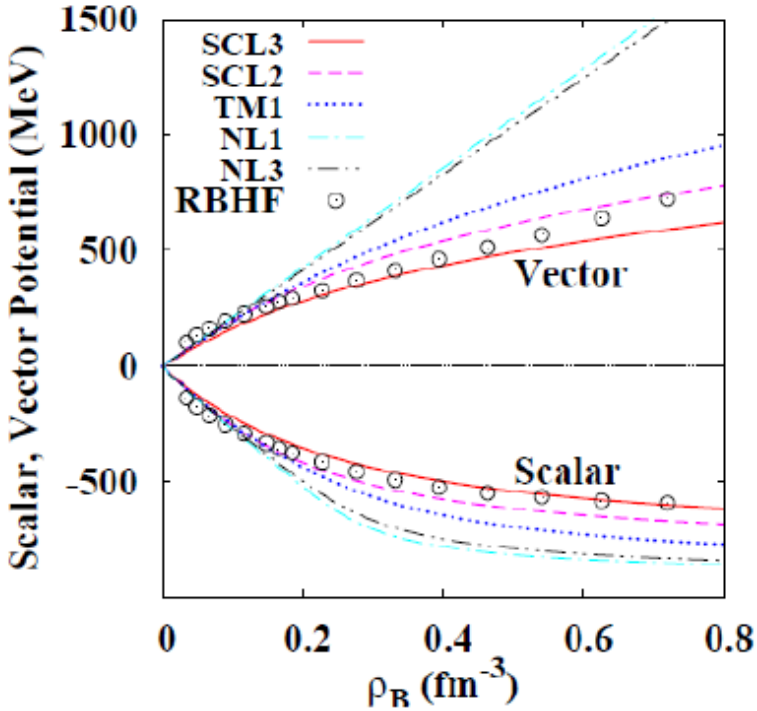

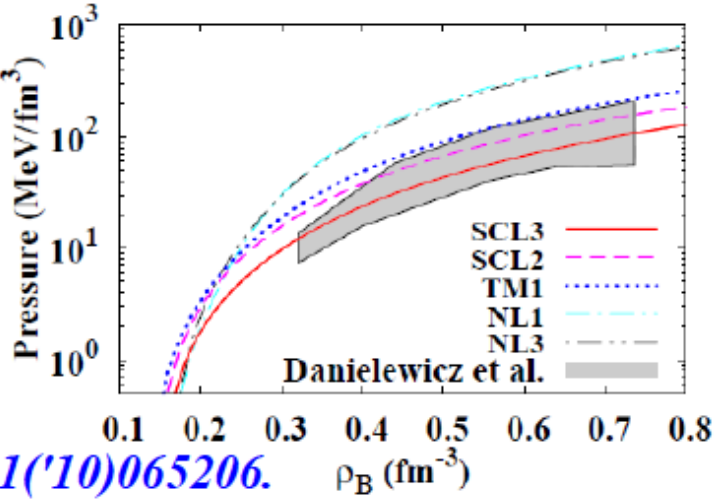

K. Tsubakihara, H. Maekawa, H. Matsumiya, AO,PRC81('10)065206.

RMF with Hyperons (Single Λ hypernuclei)

- **RMF for Λ hypernuclei**

x ~ 1/3: R. Brockmann, W. Weise, PLB69('77)167; J. Boguta and S. Bohrmann, PLB102('81)93.
x ~ 2/3: N. K. Glendenning, PRC23('81)2757, PLB114('82)392;
Tensor: Y. Sugahara, H. Toki, PTP92('94)803; H. Shen, F. Yang, H. Toki, PTP115('06)325; J. Mares, B. K. Jennings, PRC49('94)2472.
ρ-dep. coupling: H. Lenske, Lect. Notes Phys. 641('04)147; C. M. Keil, F. Hofmann, H. Lenske, PRC 61('00)064309.
SU(3) or SU(6) (ς, φ): J. Schaffner, C. B. Dover, A. Gal, C. Greiner, H. Stoecker,PRL71('93)1328; Schaffner et al., Ann.Phys.235('94)35; J. Schaffner, I. N. Mishustin, PRC 53('96)1416.
Chiral SU(3) RMF: K. Tsubakihara, H. Maekawa, H. Matsumiya, AO, PRC81('10)065206.

- **Sep. E. of Λ is well fitted by $U_\Lambda \sim -30$ MeV $\sim 2/3\ U_N$**
- **Coupling with mesons**
  $x_M = g_{M\Lambda}/g_{MN}$
  quark counting: $x_\sigma \sim 2/3$
  π exchanges: $x_\sigma \sim 1/3$
  → Which is true ?

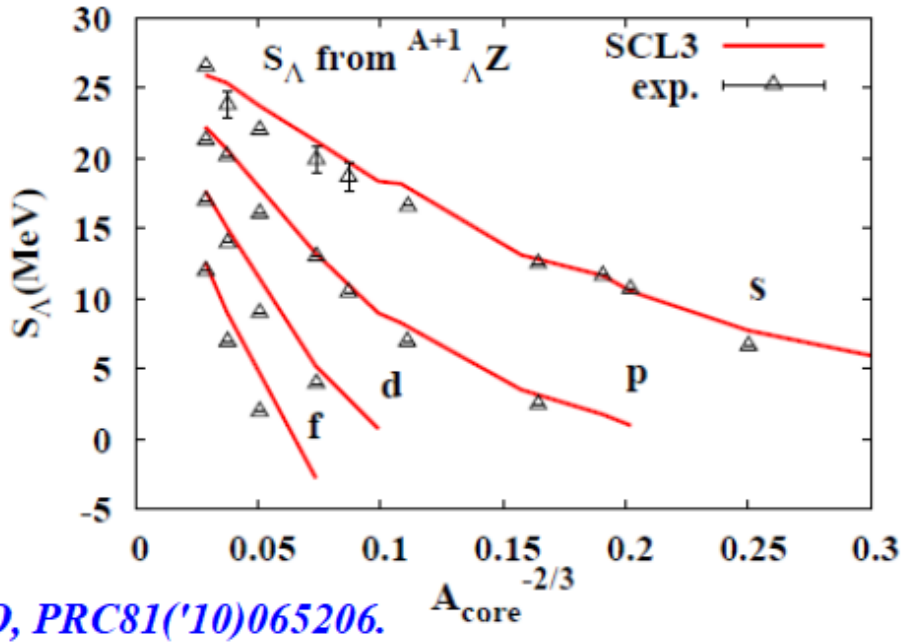

K. Tsubakihara, H. Maekawa, H. Matsumiya, AO, PRC81('10)065206.

Hyperon effect on EoS and Neutron Stars

PHYSICAL REVIEW C **85**, 025806 (2012)

Hyperon effects in covariant density functional theory and recent astrophysical observations

Wen Hui Long (龙文辉),[1,2,*] Bao Yuan Sun (孙保元),[1] Kouichi Hagino,[2] and Hiroyuki Sagawa[3]

Chemical equilibrium condition

$$\mathscr{L}_\Lambda = \bar{\psi}_\Lambda (i\gamma^\mu \partial_\mu - M_\Lambda - g_{\sigma\text{-}\Lambda}\sigma - g_{\omega\text{-}\Lambda}\gamma^\mu \omega_\mu)\psi_\Lambda,$$

$$g_{\sigma\text{-}\Lambda}/g_\sigma = 0.600 \text{ and } g_{\omega\text{-}\Lambda}/g_\omega = 0.653 \text{ [}$$

$$\mu_p = \mu_n - \mu_e,$$
$$\mu_\Lambda = \mu_n,$$
$$\mu_\mu = \mu_e,$$

$$M_\Lambda = 1115.0 \text{ MeV}, m_e = 0.511 \text{ MeV}, \text{and } m_\mu = 105.7 \text{ MeV},$$

TABLE I. Details of the selected CDF effective Lagrangians.

	Fock term	Nonlinear σ term	Nonlinear ω term	Density-dependent couplings
PKA1	yes	no	no	yes
PKO3	yes	no	no	yes
NLSH	no	yes	no	no
PK1	no	yes	yes	no
TW99	no	no	no	yes
PKDD	no	no	no	yes

TABLE III. Bulk properties of symmetric nuclear matter at saturation point, i.e., the saturation density ρ_0 (fm^{-3}), binding energy per particle E/A (MeV), incompressibility K (MeV), and symmetry energy J (MeV) with its slope L (MeV) and curvature K_{sym} (MeV). The results are provided by the CDF effective Lagrangians PKA1, PKO3, PKDD, TW99, NL-SH, and PK1.

	ρ_0	E/A	K	J	L	K_{sym}
PKA1	0.160	−15.83	229.96	36.02	103.50	213.23
PKO3	0.153	−16.04	262.47	32.99	83.00	116.56
PKDD	0.150	−16.27	262.18	36.79	90.21	−80.74
TW99	0.153	−16.25	240.27	32.77	55.31	−124.68
NL-SH	0.146	−16.35	355.43	36.12	113.66	79.72
PK1	0.148	−16.27	282.69	37.64	115.88	55.33

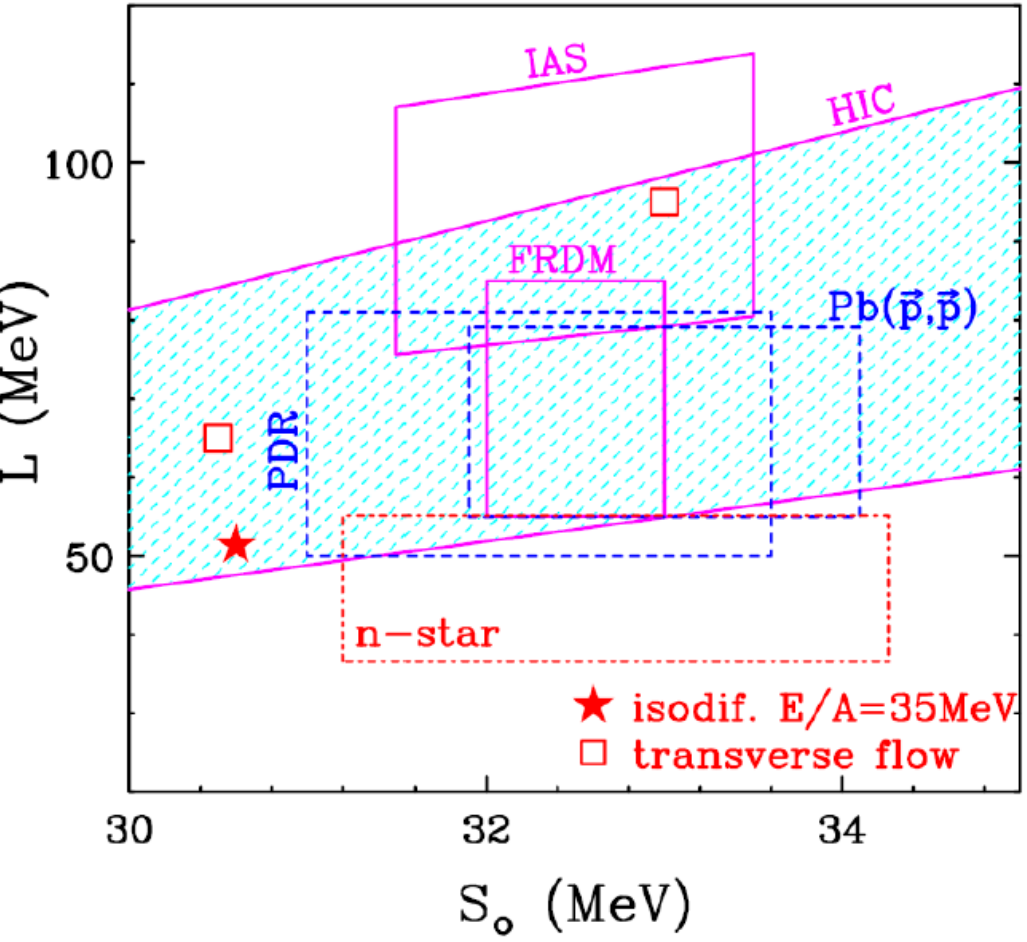

Constraints on the symmetry energy and neutron skins from experiments and theory

M.B. Tsang[1], J. R. Stone[2], F. Camera[3], P. Danielewicz[1], S. Gandolfi[4], K. Hebeler[5], C. J. Horowitz[6], Jenny Lee[7], W.G. Lynch[1], Z. Kohley[1], R. Lemmon[8], P. Moller[4], T. Murakami[9], S. Riordan[10], X. Roca-Maza[11], F. Sammarruca[12], A. W. Steiner[13], I. Vidaña[14], S.J. Yennello[15]

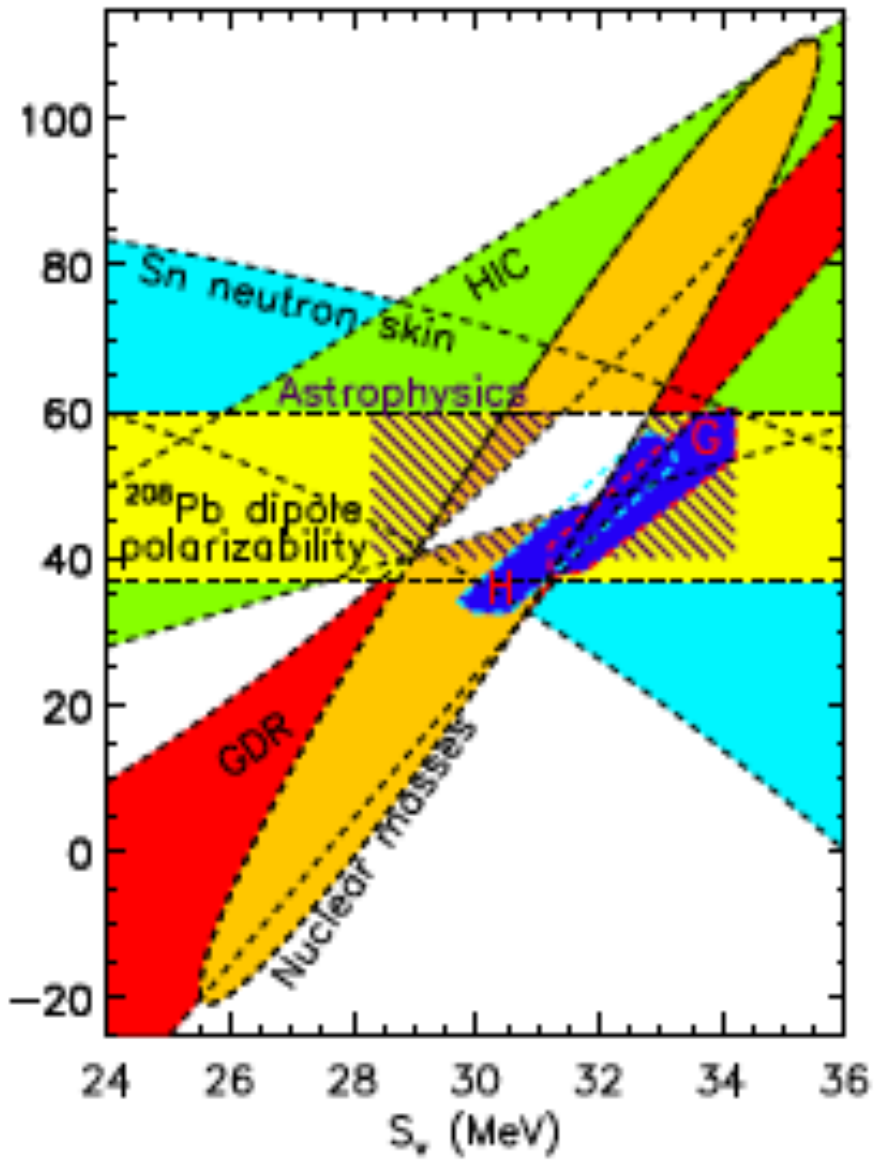

Constraining the Symmetry Parameters of the Nuclear Interaction

J. M. Lattimer[1,*] and Y. Lim[1,†]

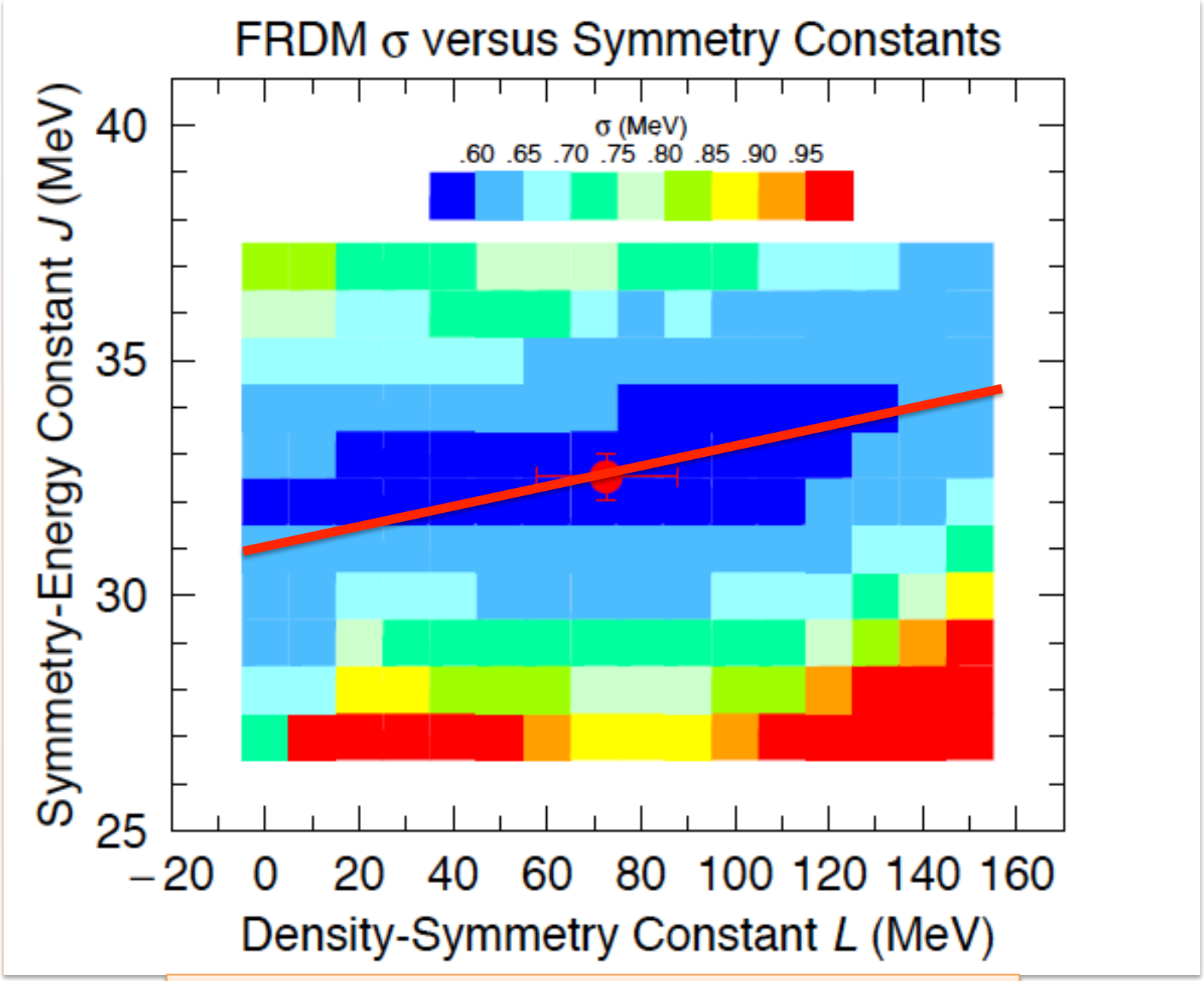

J=32.5+/-0.5MeV L=70+/-15MeV
(L=54+/-15MeV: better zero point fluctuation)

Determining Symmetry Parameters from Nuclear Masses

From liquid drop model:

$$E_{\rm sym}(N,Z) = (S_v A - S_s A^{2/3}) I^2$$

$$\chi^2 = \sum_i (E_{ex,i} - E_{sym,i})^2 / \mathcal{N}\sigma_D^2$$

$$\chi_{vv} = \frac{2}{\mathcal{N}\sigma_D^2} \sum_i I_i^4 A_i^2$$

$$\chi_{ss} = \frac{2}{\mathcal{N}\sigma_D^2} \sum_i I_i^4 A_i^{4/3}$$

$$\chi_{vs} = \frac{2}{\mathcal{N}\sigma_D^2} \sum_i I_i^4 A_i^{5/3}$$

$$\sigma_{S_v} = \sqrt{\frac{2\chi_{ss}}{\chi_{vv}\chi_{ss} - \chi_{sv}^2}} \simeq 2.3\,\sigma_D$$

$$\sigma_{S_s} = \sqrt{\frac{2\chi_{vv}}{\chi_{vv}\chi_{ss} - \chi_{sv}^2}} \simeq 13.2\,\sigma_D$$

$$\alpha = \frac{1}{2}\tan^{-1}\frac{2\chi_{vs}}{\chi_{vv} - \chi_{ss}} \simeq 9°.8$$

$$r_{vs} = -\frac{\chi_{vs}}{\sqrt{\chi_{vv}\chi_{ss}}} \simeq 0.997$$

Liquid droplet model:

$$E_{\rm sym}(N,Z) = \frac{S_v A I^2}{1 + (S_s/S_v) A^{-1/3}}$$

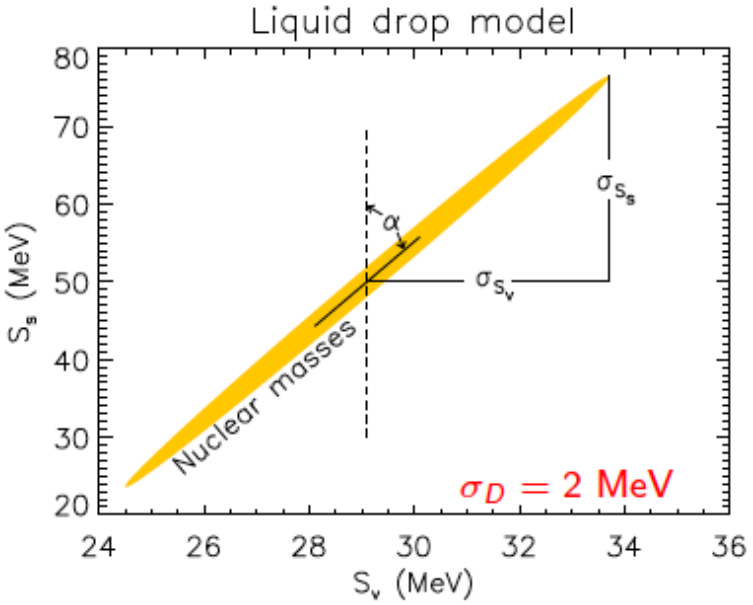

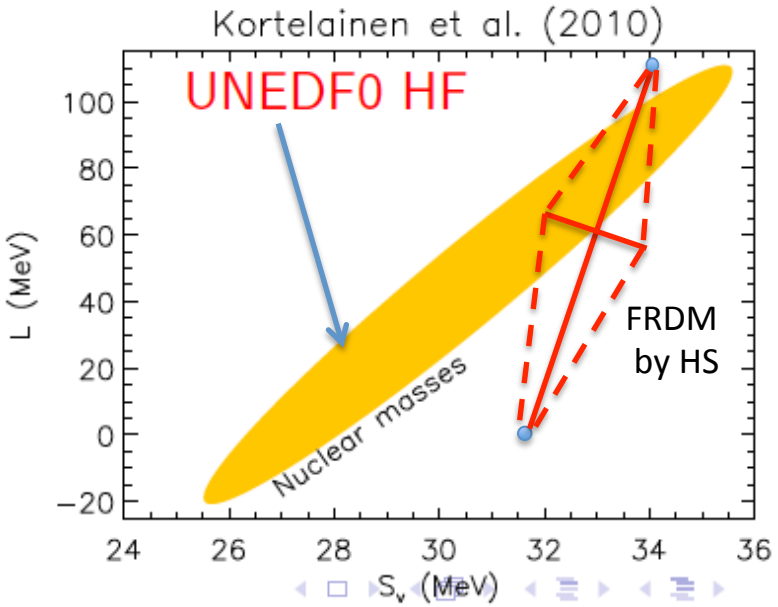

PHYSICAL REVIEW C **85**, 025806 (2012)

Hyperon effects in covariant density functional theory and recent astrophysical observations

Wen Hui Long (龙文辉),[1,2,*] Bao Yuan Sun (孙保元),[1] Kouichi Hagino,[2] and Hiroyuki Sagawa[3]

$$\mathscr{L}_\Lambda = \bar{\psi}_\Lambda(i\gamma^\mu\partial_\mu - M_\Lambda - g_{\sigma\text{-}\Lambda}\sigma - g_{\omega\text{-}\Lambda}\gamma^\mu\omega_\mu)\psi_\Lambda, \quad (1)$$

where M_Λ denotes the mass of the Λ hyperon (ψ_Λ). From the Lagrangian density (1) the contributions to the energy functional as well as the Dirac equation for the Λ hyperon can be determined as for the nucleon [9,11,16,28].

For the β-stable stellar matter containing nucleons, Λ hyperons, electrons, and muons, the chemical equilibrium conditions require that

$$\mu_p = \mu_n - \mu_e, \quad (2)$$

$$\mu_\Lambda = \mu_n, \quad (3)$$

$$\mu_\mu = \mu_e, \quad (4)$$

where the chemical potentials μ_n, μ_p, μ_Λ, μ_μ, and μ_e are determined by the relativistic energy-momentum relation at Fermi momentum $p = k_F$ [9],

$$\mu_i = \Sigma_0(k_{F,i}) + E^*(k_{F,i}), \quad \mu_\lambda = \sqrt{k_{F,\lambda}^2 + m_\lambda^2}. \quad (5)$$

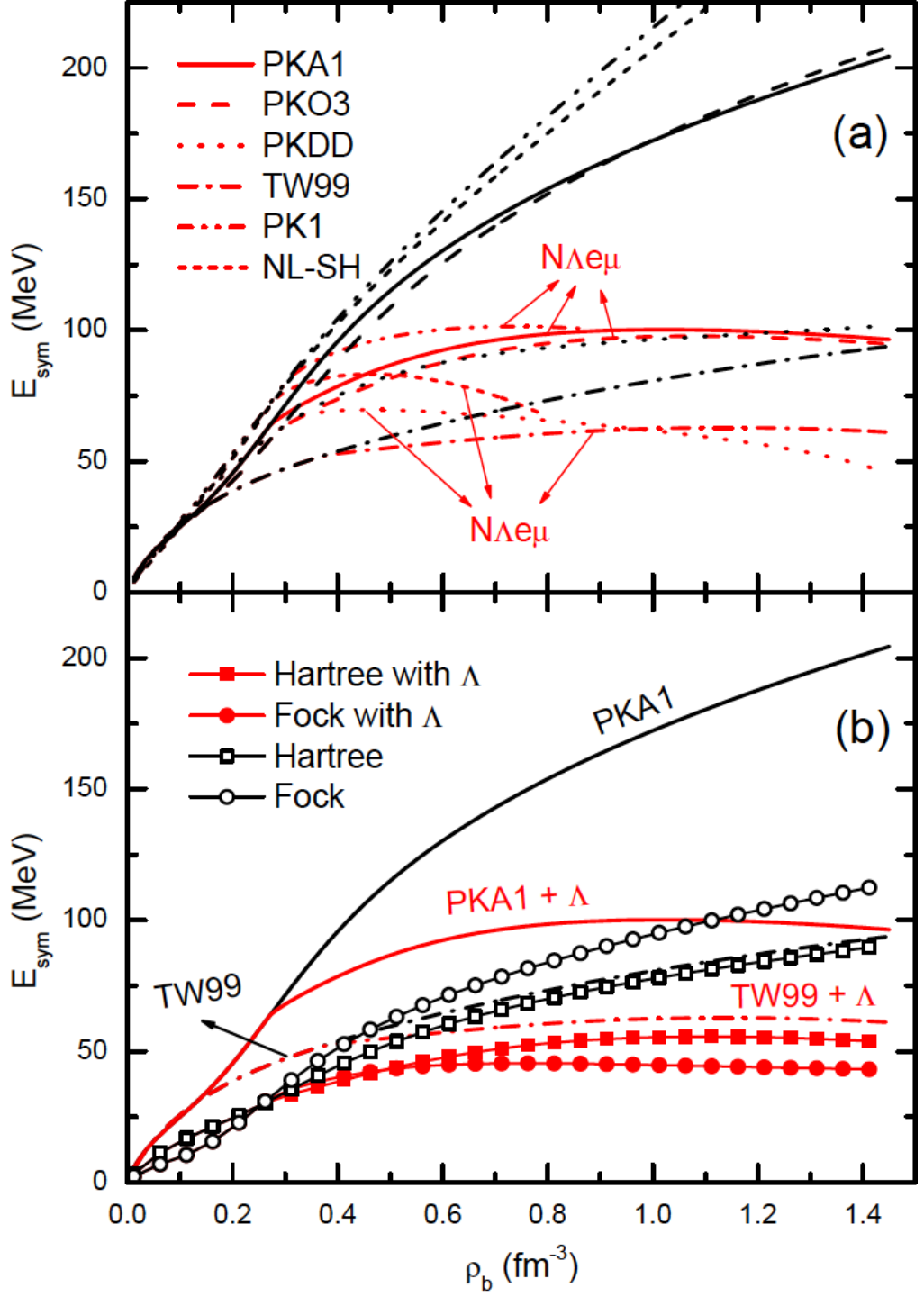
PKA1
PKO3
PKDD
TW99
PK1
NL-SH
(a)
NΛeμ
NΛeμ
E_{sym} (MeV)
Hartree with Λ
Fock with Λ
Hartree
Fock
(b)
PKA1
PKA1 + Λ
TW99
TW99 + Λ
E_{sym} (MeV)
ρ_b (fm^{-3})

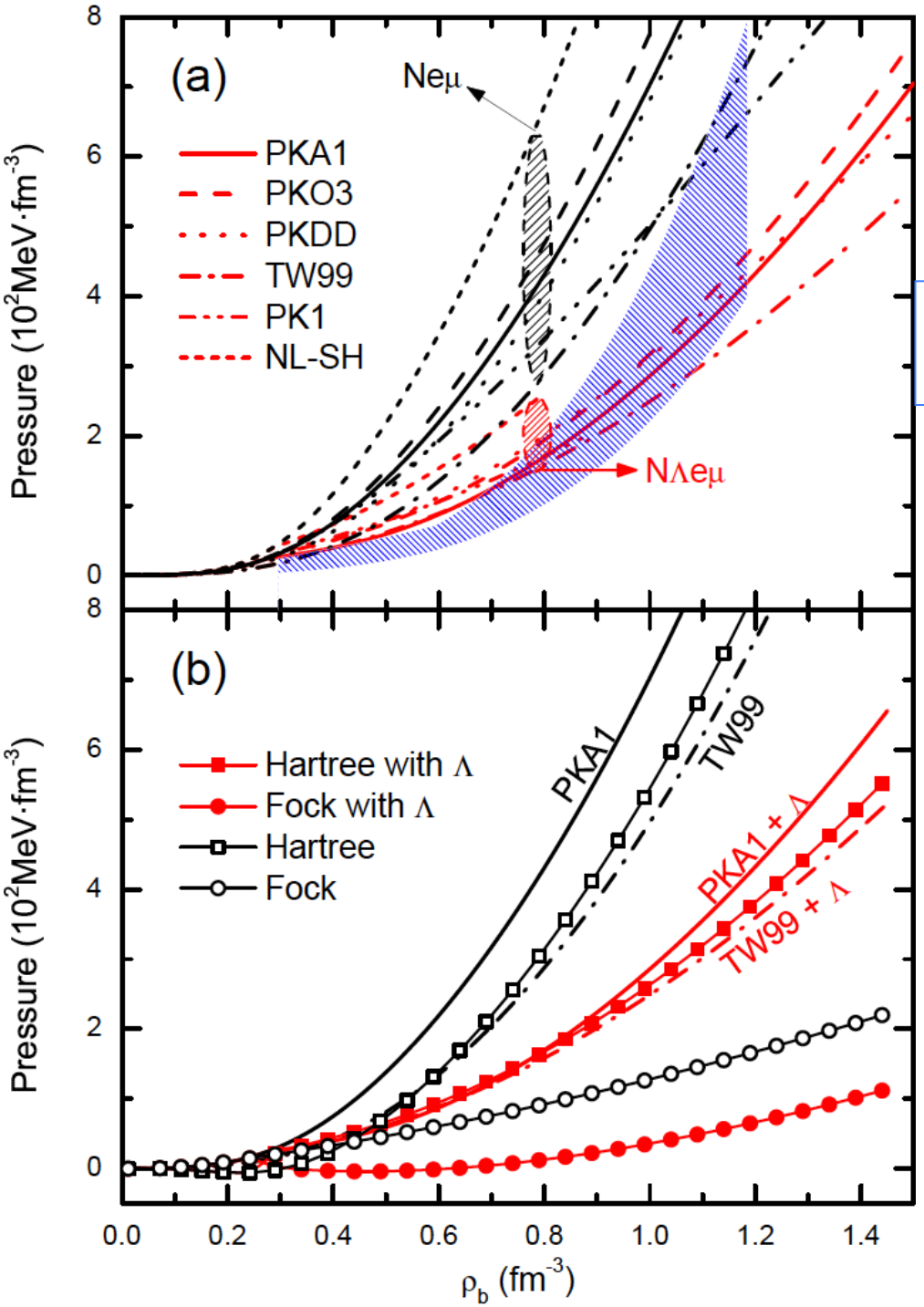

Blue Shaded area by Danielewicz

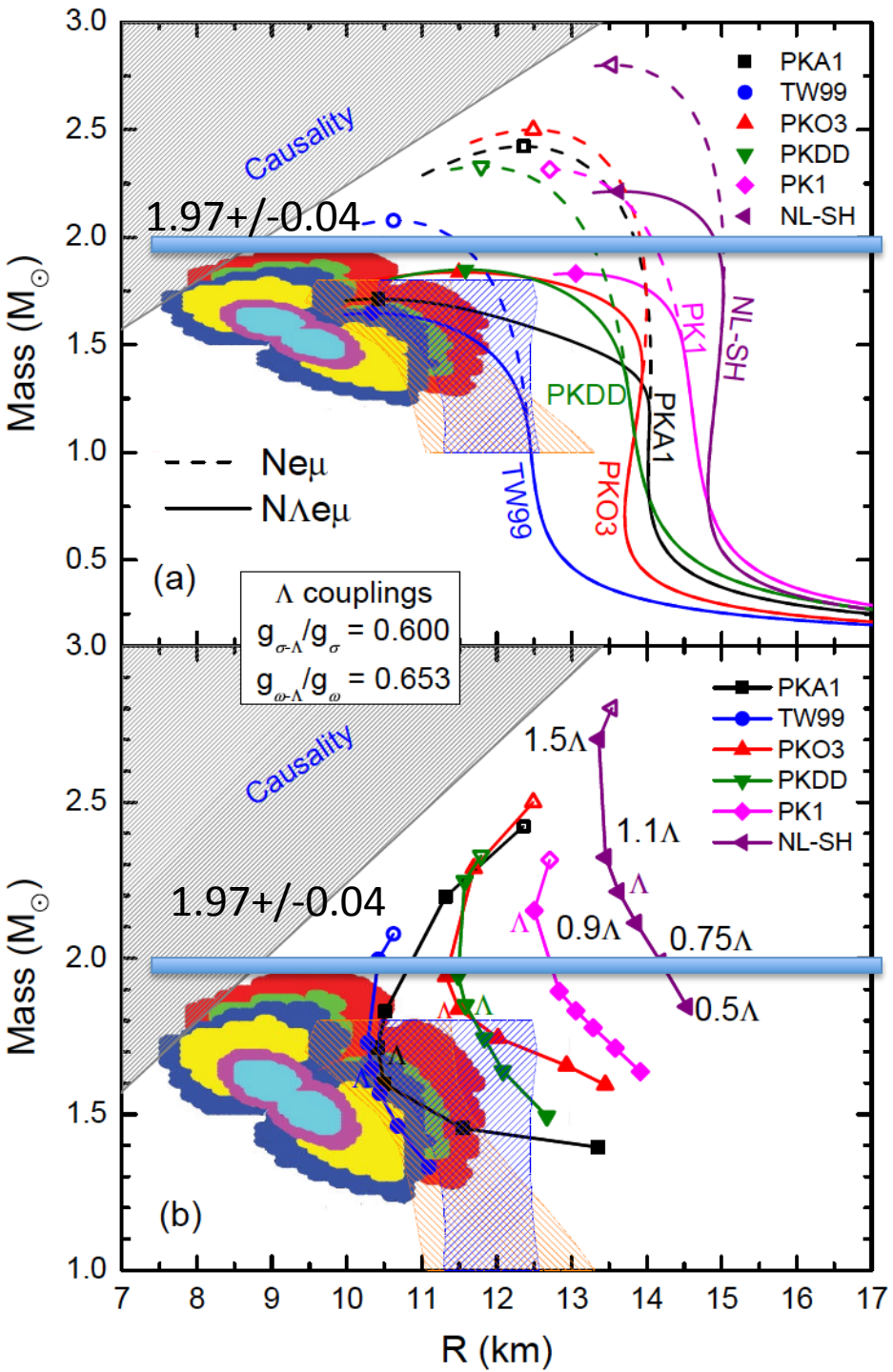

To solve Tolman-Openheimer-Volkov Eq.

TABLE II. Maximum mass M_{max} ($M_\odot$), corresponding radii R_{max} (km), and central density ρ_c (fm^{-3}) for neutron stars, as well as the threshold densities ρ_b^Λ (fm^{-3}) and ρ_b^μ (fm^{-3}) of Λ and muon emergence. For comparison, the quantities for neutron stars without Λ hyperons are shown in the last three rows. The results are calculated by DDRHF with PKA1 and PKO3 and RMF with PKDD, TW99, PK1, and NL-SH.

	PKA1	PKO3	PKDD	TW99	PK1	NL-SH
M_{max}	1.713	1.837	1.849	1.647	1.832	2.213
R_{max}	10.425	11.495	11.583	10.333	13.048	13.633
ρ_c	1.314	1.048	1.024	1.292	0.786	0.700
ρ_b^Λ	0.272	0.284	0.322	0.368	0.306	0.282
ρ_b^μ	0.118	0.122	0.108	0.116	0.110	0.114
M_{max}	2.423	2.500	2.329	2.078	2.315	2.802
R_{max}	12.354	12.487	11.798	10.632	12.705	13.534
ρ_c	0.810	0.780	0.888	1.104	0.796	0.650

FIG. 3. (Color online) (a) The mass-radius relations for the neutron stars with Λ hyperons (solid lines) and without Λ hyperons (dashed lines). The symbols denote the neutron stars with maximum masses. The region excluded by causality is shaded. For comparison the observational constraints from three neutron stars in the binaries 4U 160-8248 (light gray/white gray), EXO 1745-248 (dark gray/gray), and 4U 1820-30 (black/black gray) in Ref. [12] are shown as the 1σ and 2σ confidence contours, and the later analyses in Ref. [13] are denoted by the shaded areas with two different models of photospheric radius. (b) The mass and radius for the neutron stars with maximum masses determined with different Λ-hyperon coupling strengths (solid symbols), compared to the ones without Λ hyperons (open symbols). See the text for details.

Ref. 12 E. Ozel et al., Phys. Rev. D82, 101301(R) (2010).
13 A. W. Steiner et al., Atrophys. J722, 33 (2010).

Bruckner-Hartree-Fock theory with Hyperons

- **Microscopic G-matrix calculation with realistic NN, YN potential and microscopic (or phen.) 3N force (or 3B force).**
  - **Interaction dep. (V18, N93, ...) is large → Need finite nuclear info.**
    E.Hiyama, T.Motoba, Y.Yamamoto, M.Kamimura / M.Tamura et al.
  - **NS collapses with hyperons w/o 3BF.**

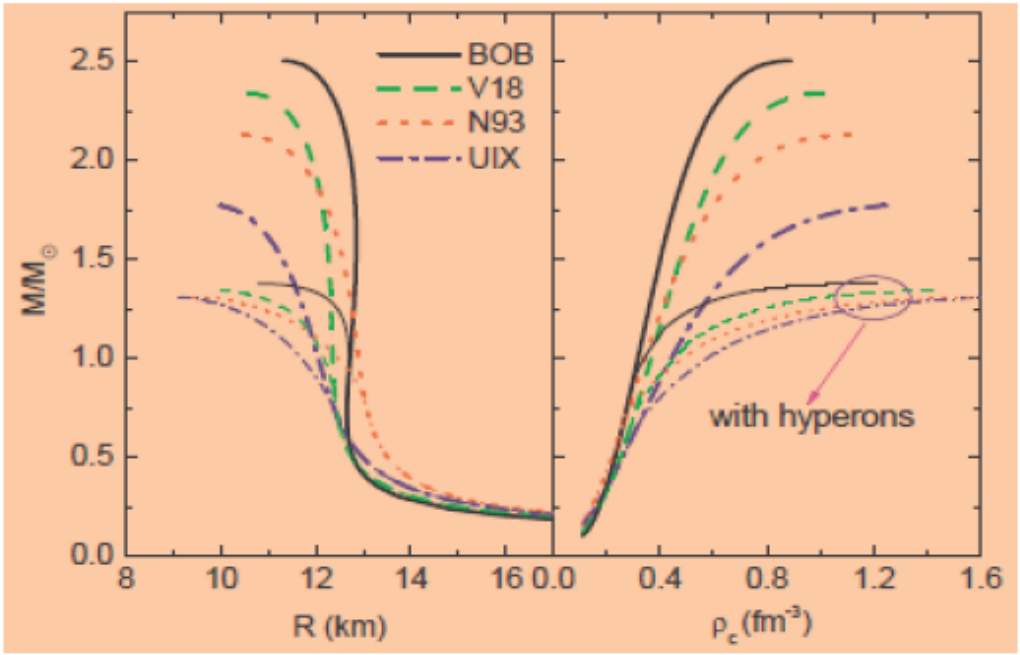

H.J.Schulze, A.Polls, A.Ramos, I.Vidana, PRC73('06),058801.

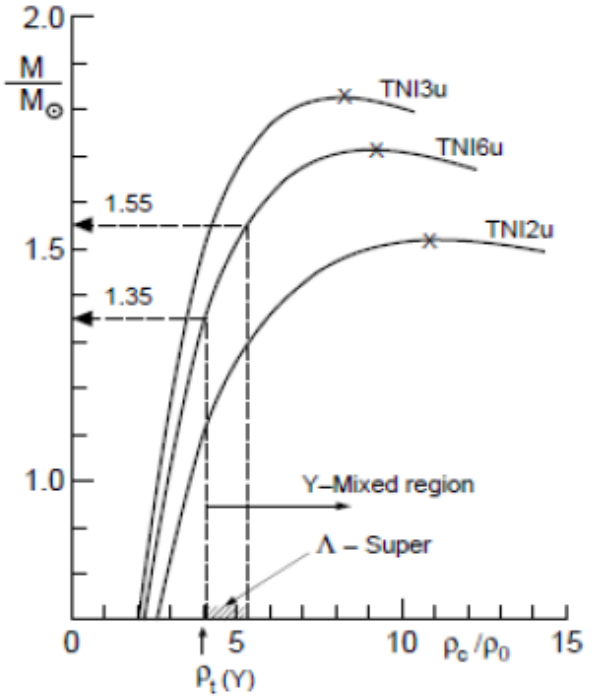

S. Nishizaki, T. Takatsuka, Y. Yamamoto, PTP108('02)703.

Courtesy of Akira Onishi

Phenomenological modeling of Three-Body Repulsion in ESC04

ESC : Modern Version of Nijmegen Potential

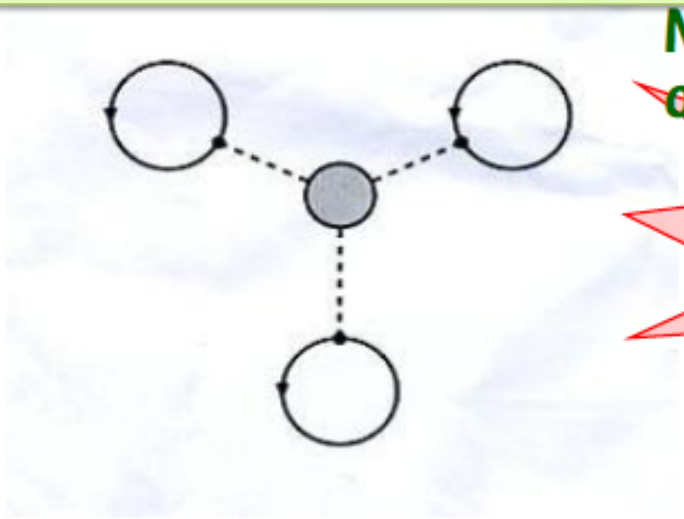

Necessary for maximum mass of neutron star

Universal among NNN, NNY, NYY…

Three-body force due to triple-meson correlation

➡ Reduction of meson mass in medium

$M_V(\rho)=M_V \exp(-\alpha\rho)$ for vector mesons

Courtesy of Yamamoto

Medium-Induced Repulsion

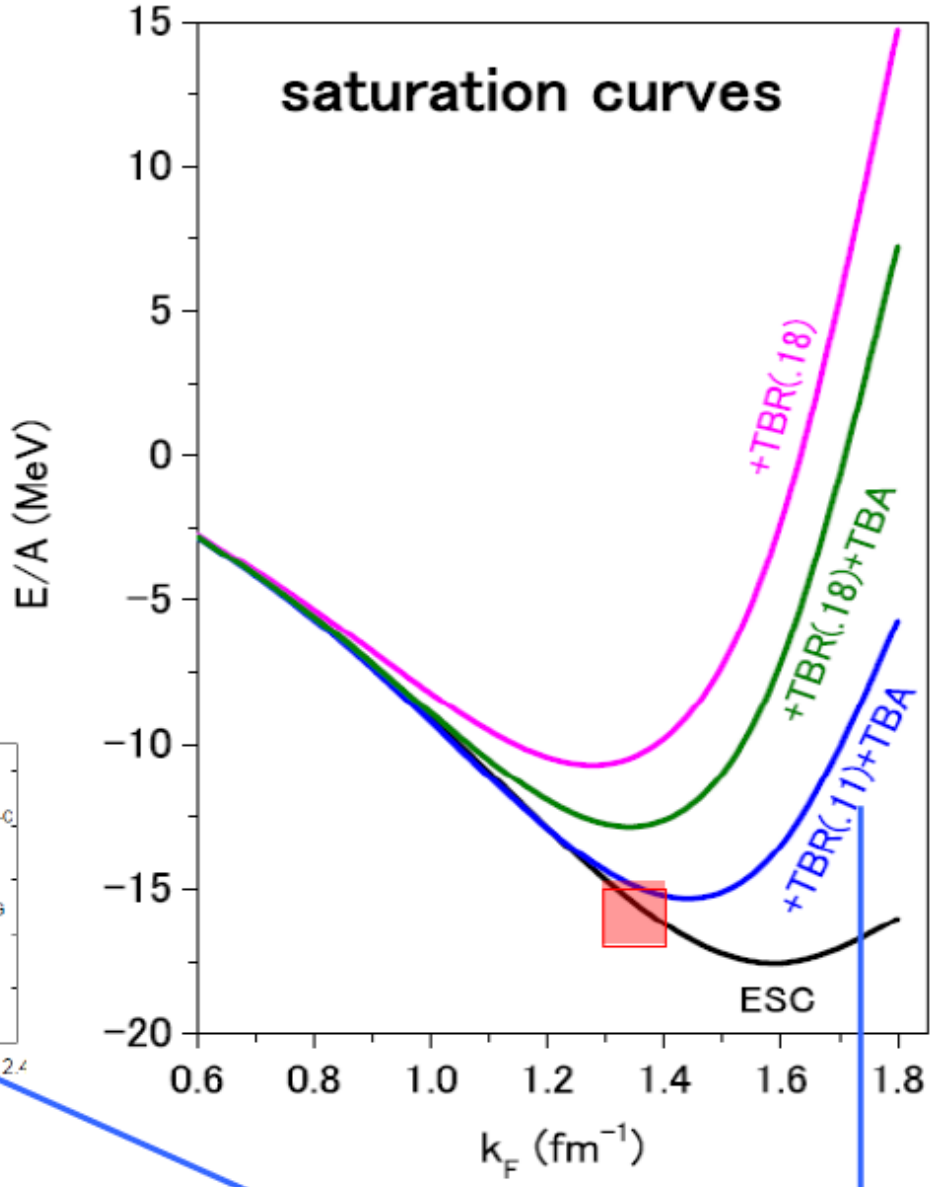

TBA

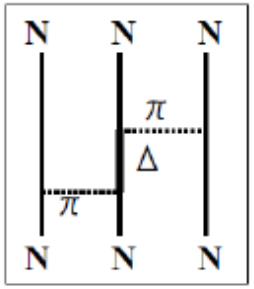

TBR

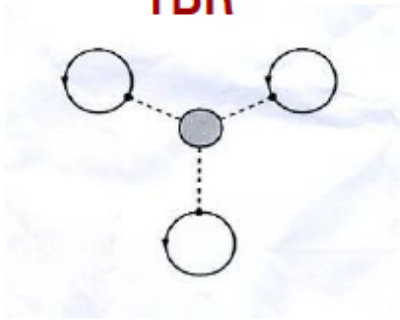

Baldo

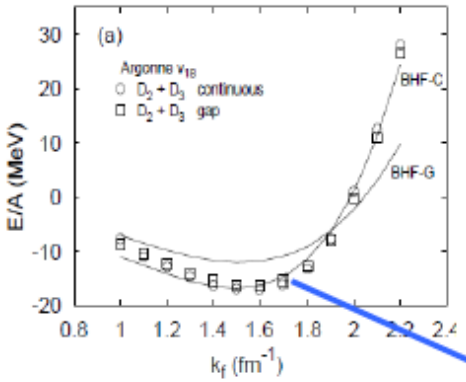

Similar curve is obtained

Univ. 3-body force → higher ρ_t(Y)

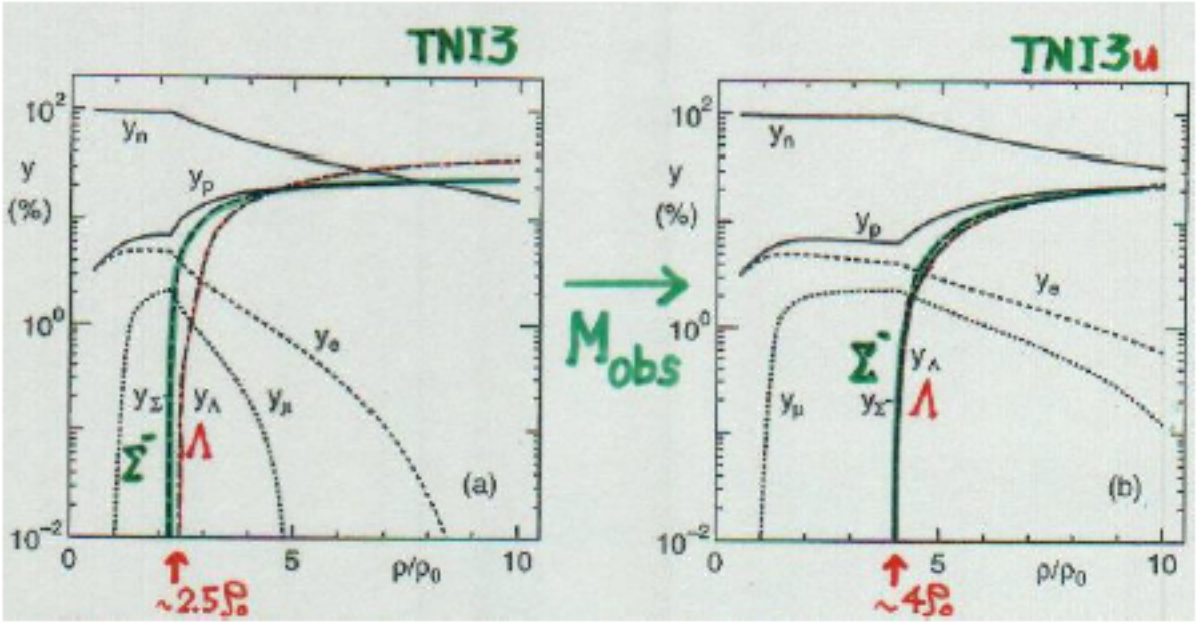

→ Y-mixed star
for $M > M_\odot$

→ Y-mixed star
for $M > 1.4M_\odot$

Maximum Mass problems in Neutron Stars

S. Nishizaki, Y. Yamamoto and T. Takatsuka

Dramatic softening of EOS ⟶ Necessity of "Extra Repulsion"

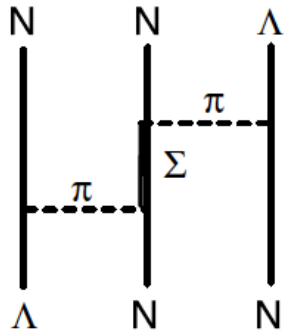

Figure 43: Three-body force caused by ΛN-ΣN coupling. It is not incorporated in the effective two-body ΛN interaction and has to be studied for each hypernucleus.

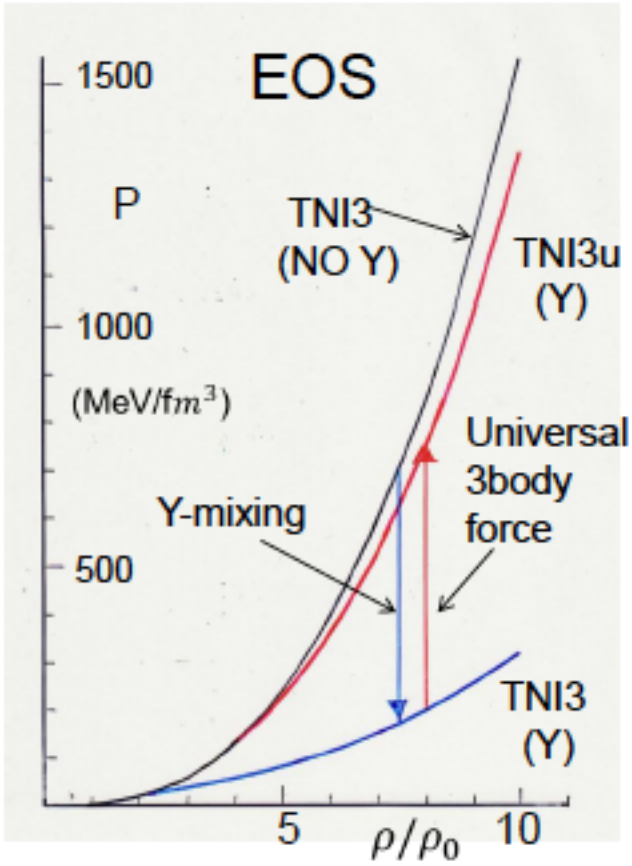

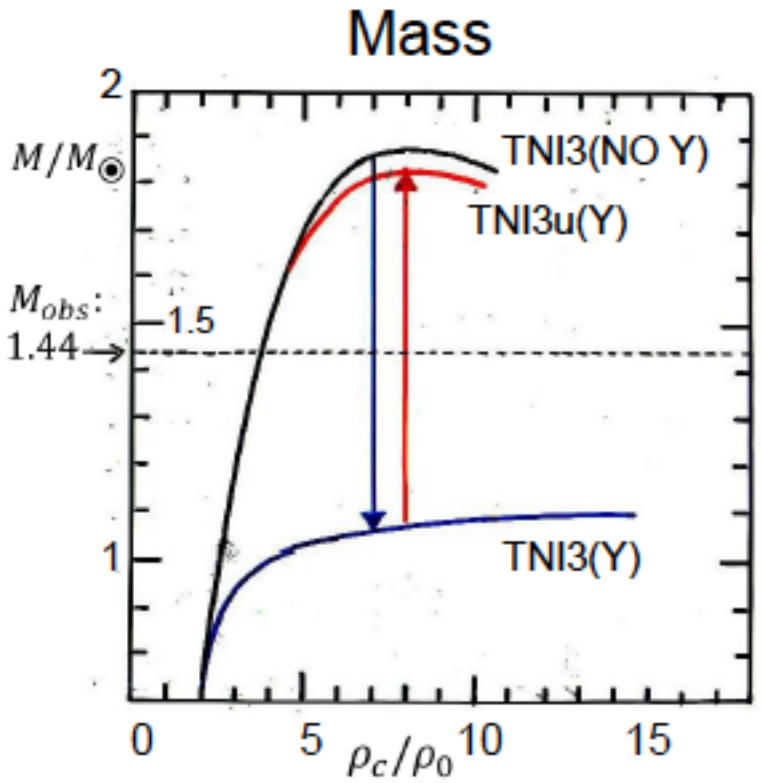

TNI3 ⟶ TNI3u: Universal inclusion of TNI3 repulsion

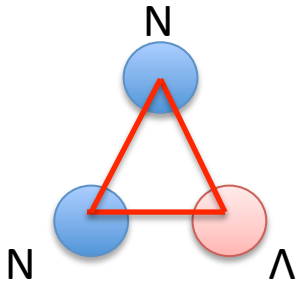

NNY repulsive interaction

RMF with 3BF

- **Three-baryon coupling term**

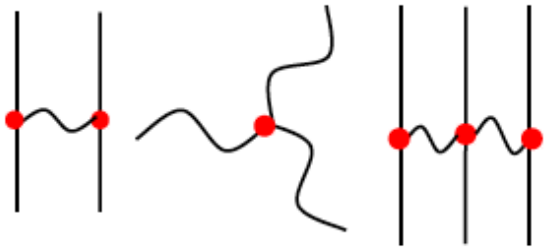

$$L = L_B^{\text{free}} + L_M^{\text{free}} + L_{BM} + L_M^{\text{Int}} + \delta L$$

$$\delta L = -U_\sigma(\sigma) - \frac{1}{2} c_{\sigma\omega} \sigma \omega_\mu \omega^\mu - \frac{1}{4} c_{\omega\omega} (\omega_\mu \omega^\mu)^2$$

$$- \sum_B \bar{\psi}_B \left[g_{\sigma\sigma B} \sigma^2 + g_{\sigma\omega B} \sigma \omega_\mu \gamma^\mu + g_{\omega\omega B} \omega_\mu \omega^\mu \right] \psi_B$$

ν = 3 terms

- **BBMM terms are ignored in standard RMF.**
  (They can be absorbed in other terms by field re-definitions.)
  R.D.Furnstahl, B.D.Serot, H.-B. Tang, NPA615 ('97)441
- **But field re-definition modifies the order of NDA.**
  Naïve dimensional analysis (NDA)
  ν = B/2 + M + d
  (B, M, d=# of baryon and non-NG boson field, derivatives to NG fields)
- **Higher ν terms are found to be suppressed at ρ ~ ρ0, but they will contribute more at high densities.**

Courtesy of Akira Onishi

RMF with 3BF + $SU(3)_f$ "violation"

Tsubakihara, AO, in prep.

- **Two types of modification**
  - **3-baryon repulsion → EOS becomes stiff gradually at high density. (Fitting meson mass (E325) and Uv in RBHF)**
  - **R= $g_{\omega\Lambda}$ / $g_{\omega N}$ ~ 0.8 (~ 2/3 (SU(3))**

→ M_{max} ~ 1.7 $M_\odot$ with hyperons (~ 1.4 $M_\odot$ w/o 3BF, violation)

T. Tsubakihara, A. Ohnishi / Nuclear Physics A 00 (2013) 1–4

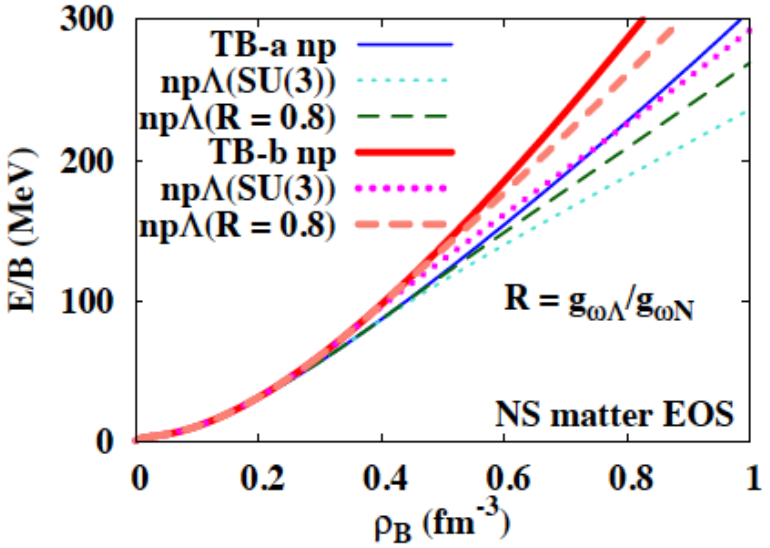

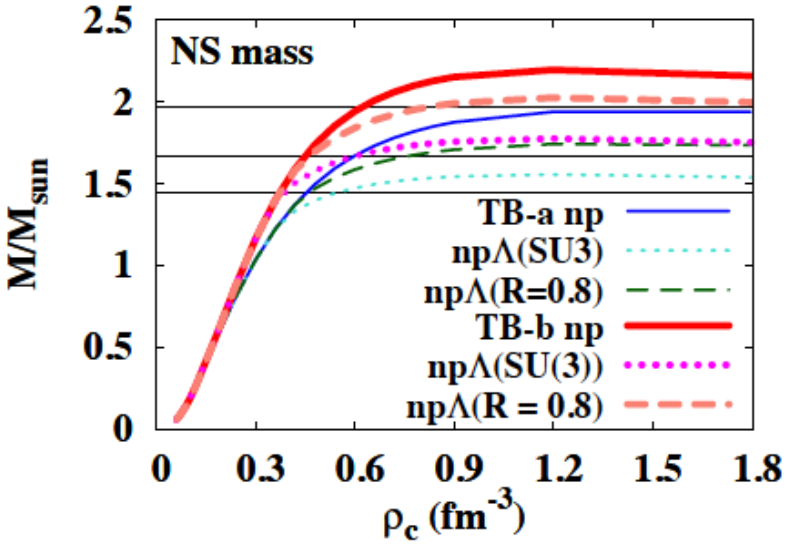

e 3. Neutron star matter EOSs as functions of ρ_B and neutron star maximum masses as functions of the central density.

Summary

- YN interaction is now studied well in light hypernuclei A<30
- Lambda-nucleon interaction gives medium strong attractive potential:

1/2~2/3 of nuclear mean field potential ($SU(3)_f$ might work) $g_{Y\sigma} / g_{N\sigma} = g_{Y\omega} / g_{N\omega} = 2/3$

- realistic BHF YN interaction is now available
- various RMF Lagrangian: Hartree and Hartree-Fock level
- hyperon makes softer EoS and does not support $2M_\odot$ of neutron stars
- need a repulsive three-force at high density EoS

Future perspectives

- how we can justify repulsive YNN interaction at high density?
  (theoretically and experimentally)
- YY interaction: too weak to make hyperon condensation in neutron star ?
  need more data
- quark degree of freedom => softer EoS?
  crossover to baryon to quarks => hard EoS (Hatsuda)
- cooling process of neutron star: hyperon effect?

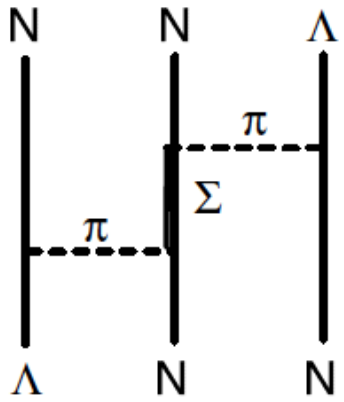

Figure 43: Three-body force caused by ΛN-ΣN coupling. It is not incorporated in the effective two-body ΛN interaction and has to be studied for each hypernucleus.

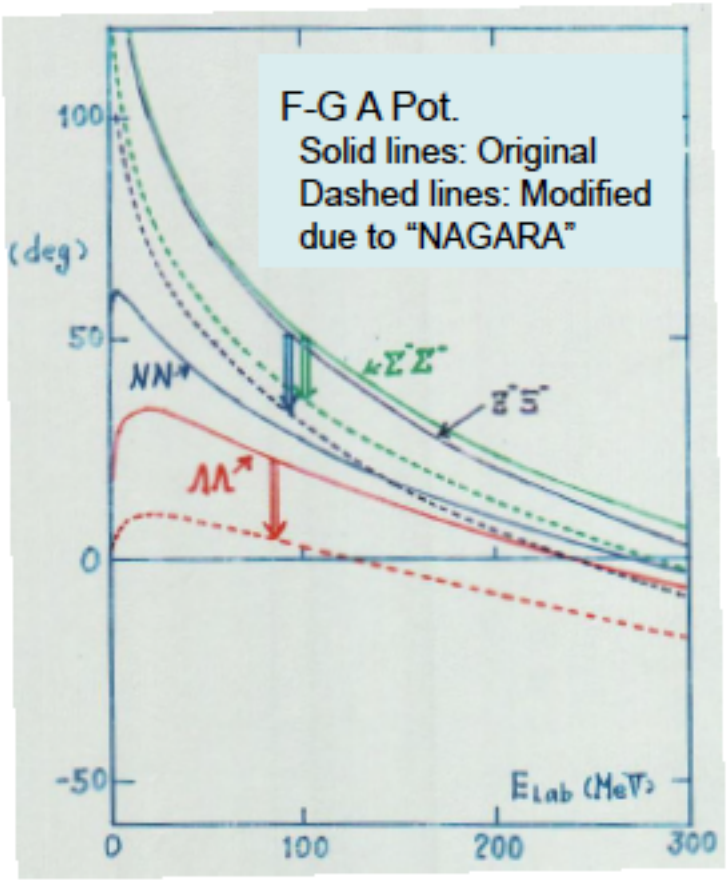

V(ND-soft)→ 0.5V(ND-soft) ; Hiyama

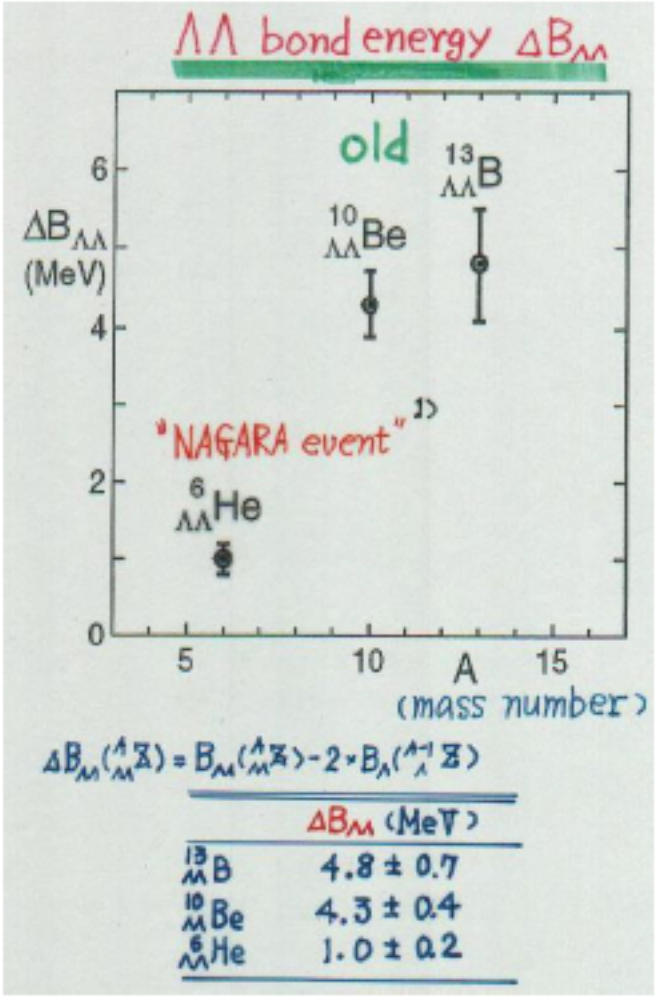

Takahashi et al., PRL 87 (2001) 212502

RMF with Hyperons (Double Λ hypernuclei)

- **Nagara event $\Delta B_{\Lambda\Lambda} \sim 1.0$ MeV (weakly attractive)**
  - **TM & NL-SH based RMF**
    H. Shen, F. Yang, H. Toki, PTP115('06)325.
    Model 1: $x_\sigma = 0.621$, $x_\omega = 2/3$ (no ς, φ)
    Model 2: $R_\varsigma = g_{\varsigma\Lambda}/g_{\sigma N} = 0.56\text{-}0.57$, $R_\varphi = g_{\varphi\Lambda}/g_{\omega N} = -\sqrt{2}/3$
  - **Chiral SU(3) RMF**
    K. Tsubakihara, H. Maekawa, H. Matsumiya, AO, PRC81('10)065206.
    SU(3)f for vector coupling
    $x_\omega = 0.64$, $R_\varphi = 0.504$
    Det. (KMT) int. mixes σ and ς
    M. Kobayashi, T. Maskawa, PTP44('70)1422; G. 't Hooft, PRD14('76)3432.
    → $x_\sigma = 0.335$, $R_\varsigma = 0.509$

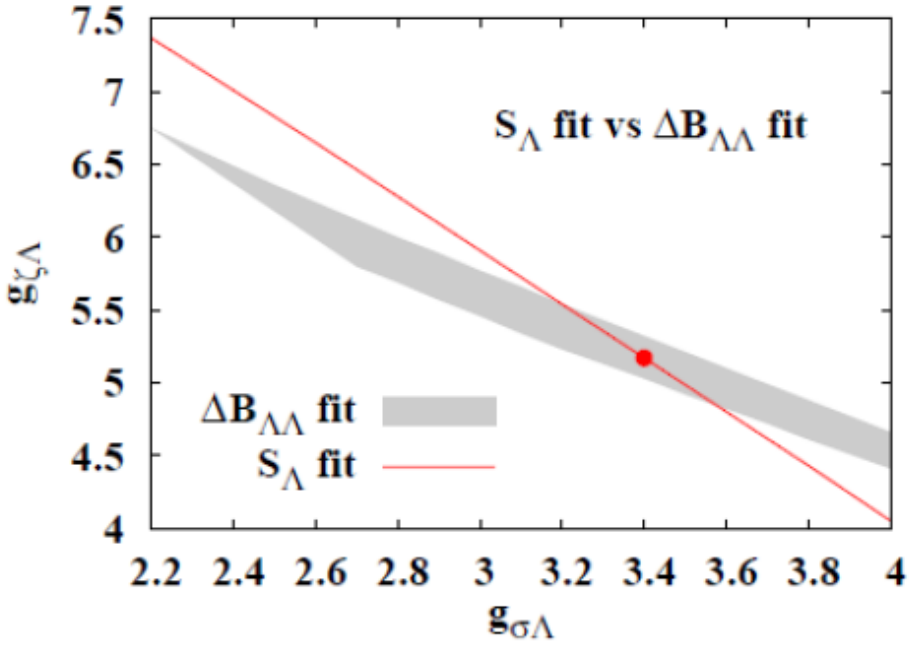

Courtesy of Akira Onishi

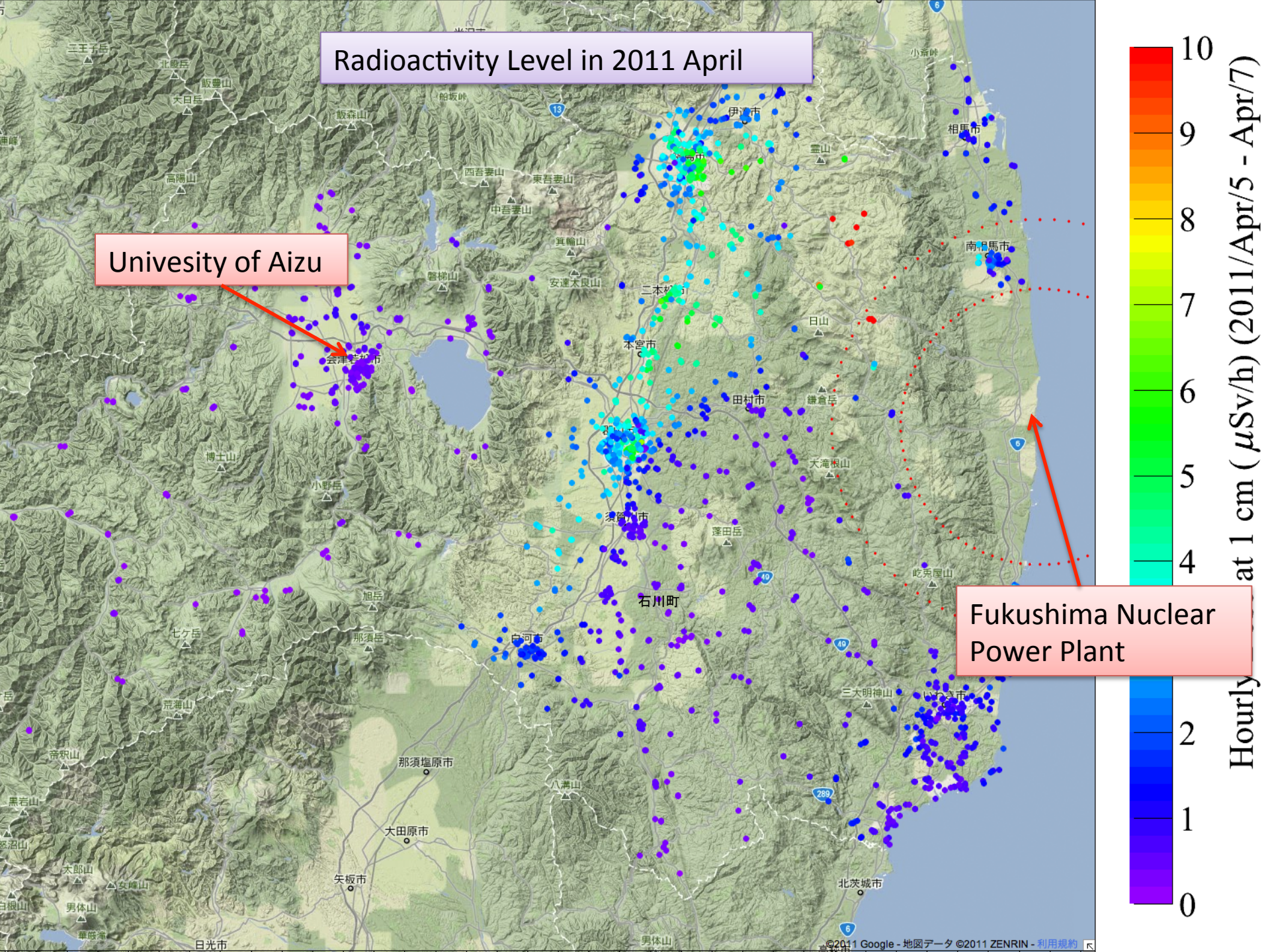
Radioactivity Level in 2011 April
Univesity of Aizu
Fukushima Nuclear Power Plant
Hourly at 1 cm (μSv/h) (2011/Apr/5 - Apr/7)
10
9
8
7
6
5
4
2
1
0
©2011 Google - 地図データ ©2011 ZENRIN - 利用規約

Three-body couplings in RMF and its effects on hyperonic star equation of state*

K. Tsubakihara[a], A. Ohnishi[b]

[a]Meme Media Laboratory, Hokkaido University.
[b]Yukawa Institute for Theoretical Physics, Kyoto University.

$$\mathcal{L}_{n=3}^{\sigma\omega} = -\frac{1}{f_\pi}\sum_B \bar{\psi}_B \left[g_{\sigma\sigma B}\sigma^2 + g_{\omega\omega B}\omega_\mu\omega^\mu - g_{\sigma\omega B}\sigma\omega_\mu\gamma^\mu \right] \psi_B - c_{\sigma\omega\omega} f_\pi \sigma\omega_\mu\omega^\mu \,. \tag{1}$$

The first and second terms modify the effective mass of nucleons, $M_N^* = M_N - (g_{\sigma N}\sigma - g_{\sigma\sigma N}\sigma^2/f_\pi - g_{\omega\omega N}\omega^2/f_\pi)$, where ω represents the temporal component. These $n = 3$ terms modify the effective mass from the $n = 2$ coupling with σ. The third term modifies the vector potential of nucleons at high density, $U_v = (g_{\omega N} - g_{\sigma\omega N}\sigma/f_\pi)\omega$, and the fourth term represents the ω meson mass shift at finite density. In RBHF calculations, the vector potential at low densities is almost proportional to the baryon density, but the vector potential to baryon density ratio U_v/ρ_B is suppressed around ρ_0 or at higher densities. This suppression in RBHF is sometimes simulated by the ω^4 term [8] or by the density dependent coupling [9]. When we simulate the suppression only with the ω^4 term, the ratio U_v/ρ_B is monotonically decreasing with increasing ρ_B. With a large coefficient of ω^4, EOS at high density is thus too softened to support the massive neutron star [7]. The density dependent vector coupling is usually chosen to decrease and be saturated with increasing ρ_B. With the present $n = 3$ coupling terms in Eq. (1) in addition to the ω^4 term, we try to simulate the decreasing and saturating behavior of the U_v/ρ_B ratio found in the RBHF results.

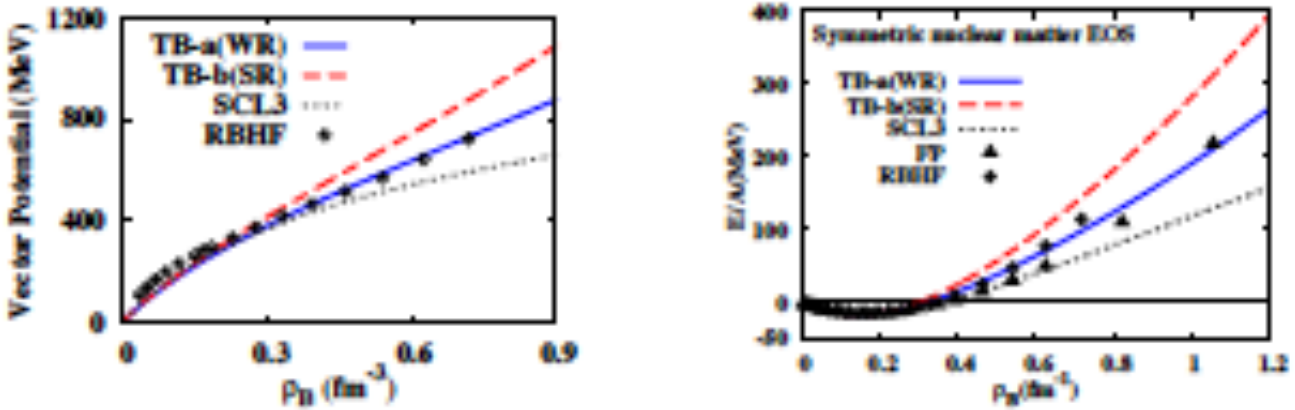

Figure 1. Calculated vector potential and EOS in symmetric nuclear matter with TB-a and TB-b parameter set in comparison with SCL3 results.

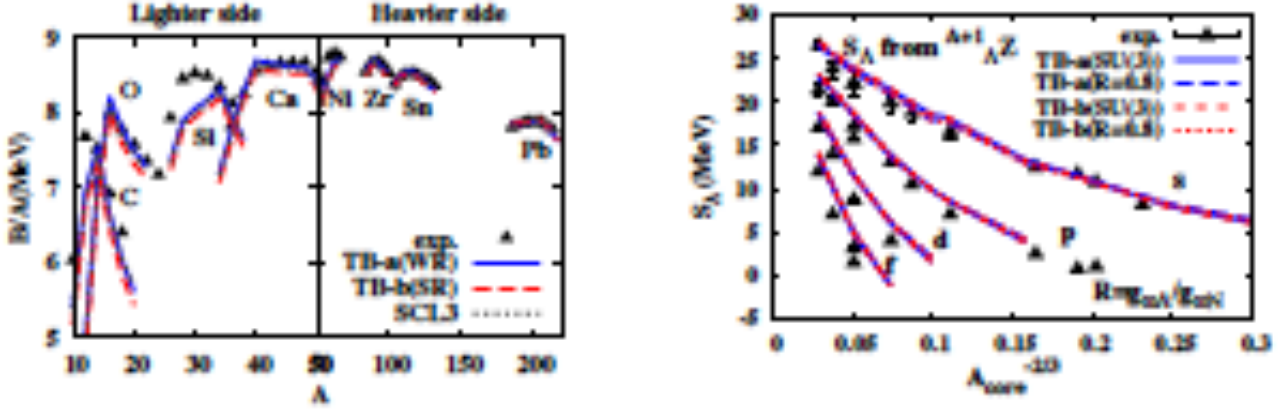

Figure 2. Calculated binding energies and A separation energies (S_A) based on TB-a and TB-b parameter sets.

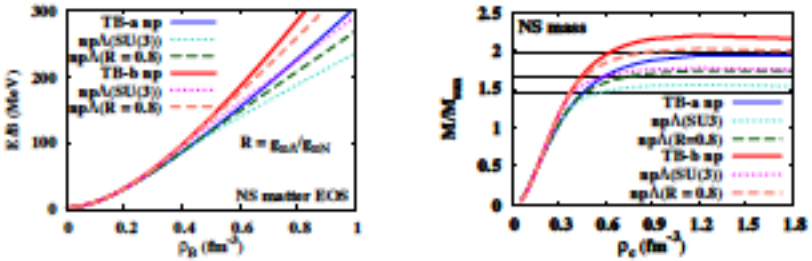

Figure 3. Neutron star matter EOSs as functions of ρ_B and neutron star maximum masses as functions of the central density.

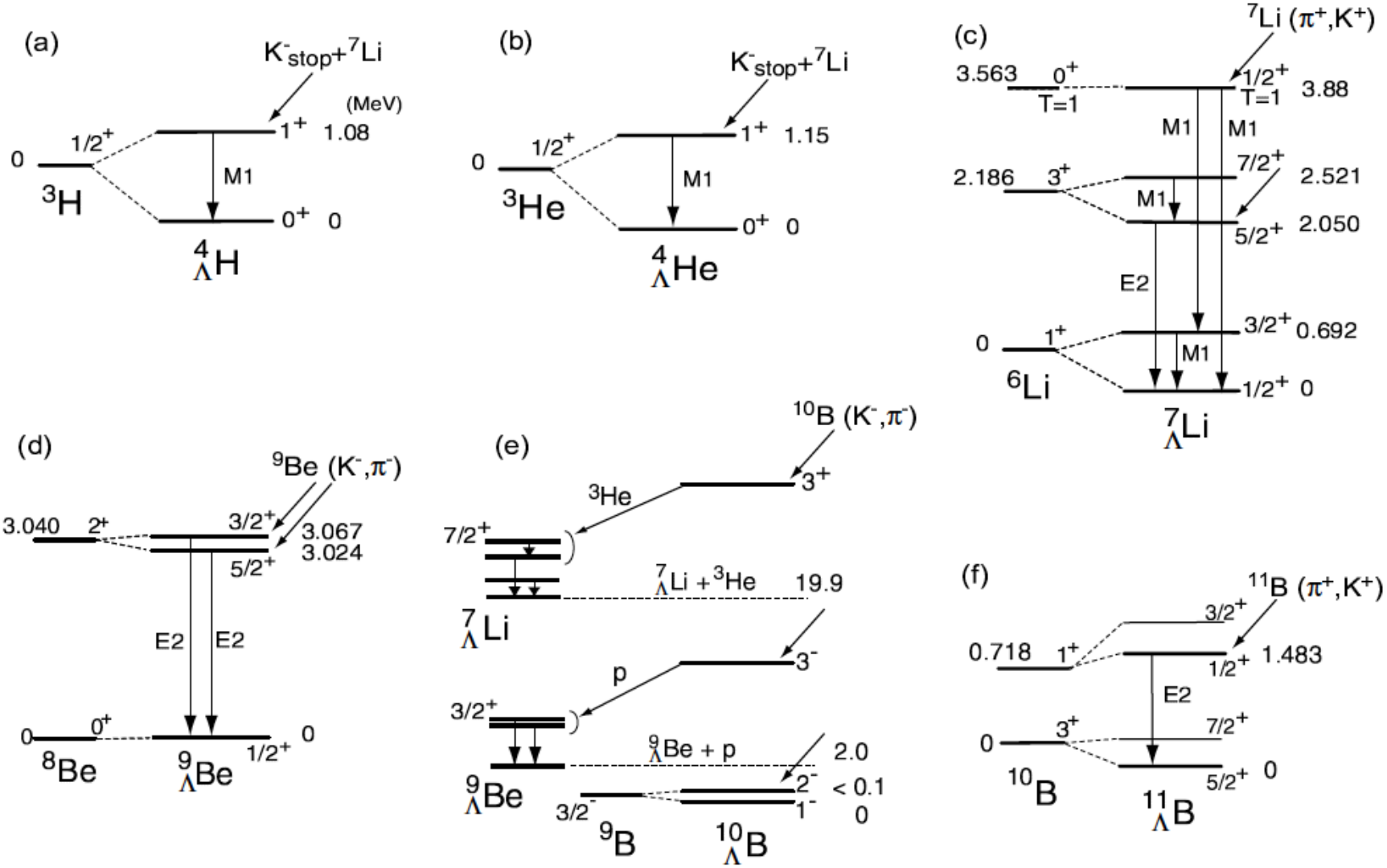
(a)
K⁻stop+⁷Li
(MeV)
1⁺ 1.08
1/2⁺
0
M1
³H
0⁺ 0
⁴ΛH
(b)
K⁻stop+⁷Li
1⁺ 1.15
1/2⁺
0
M1
³He
0⁺ 0
⁴ΛHe
(c)
⁷Li (π⁺,K⁺)
3.563 0⁺
T=1
1/2⁺ T=1 3.88
M1 M1
2.186 3⁺
7/2⁺ 2.521
M1
5/2⁺ 2.050
E2
3/2⁺ 0.692
0 1⁺
M1
6Li
1/2⁺ 0
⁷ΛLi
(d)
⁹Be (K⁻,π⁻)
3.040 2⁺
3/2⁺
3.067
3.024
5/2⁺
E2 E2
0 0⁺
0
8Be
⁹ΛBe
1/2⁺
(e)
¹⁰B (K⁻,π⁻)
3⁺
³He
7/2⁺
⁷ΛLi + ³He 19.9
⁷ΛLi
3⁻
p
3/2⁺
⁹ΛBe + p 2.0
2⁻ < 0.1
⁹ΛBe
3/2⁻
1⁻ 0
9B
¹⁰ΛB
(f)
¹¹B (π⁺,K⁺)
3/2⁺
0.718 1⁺
1/2⁺ 1.483
E2
3⁺
7/2⁺
0
10B
5/2⁺ 0
¹¹ΛB

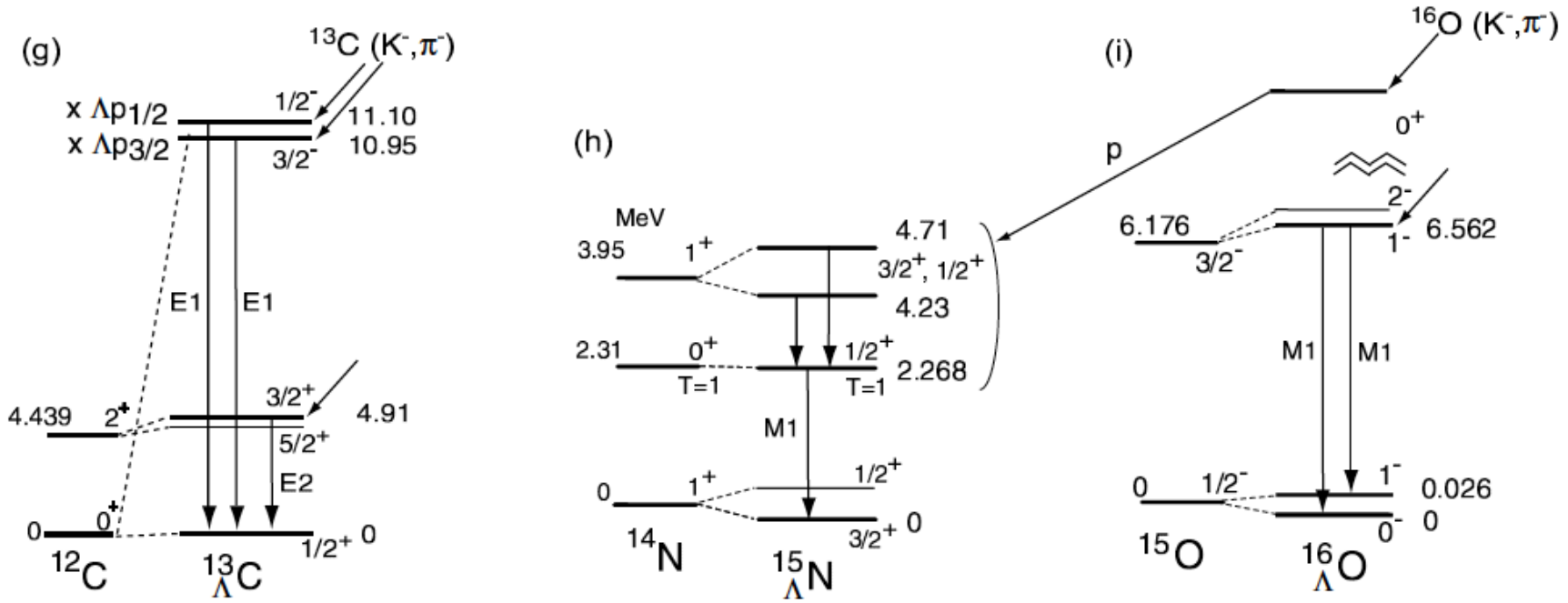

Figure 47: All the hypernuclear γ transitions observed and identified so far for $^{4}_{\Lambda}$H [33], $^{4}_{\Lambda}$He [34], $^{7}_{\Lambda}$Li [35, 25], $^{9}_{\Lambda}$Be [35, 40], $^{10}_{\Lambda}$B [36, 108], $^{11}_{\Lambda}$B [43], $^{15}_{\Lambda}$N [108], and $^{16}_{\Lambda}$O [41]. Level schemes of these hypernuclei with level energies (in MeV) and assigned spin-parities are shown together with reactions to populate excited states in γ spectroscopy experiments.